Lymphatic muscle cells are unique cells that undergo aging induced changes

Pin-Ji Lei[1,#], Katarina J. Ruscic[1,2,#], Kangsan Roh[1,3], Johanna J. Rajotte[1,4], Meghan J. O'Melia[1], Echoe M. Bouta[1], Marla Marquez[1], Ethel R. Pereira[1], Ashwin S. Kumar[1,5], Guillermo Arroyo-Ataz[6], Mohammad S. Razavi[1], Hengbo Zhou[1,7], Lutz Menzel[1], Heena Kumra[1], Mark Duquette[1], Peigen Huang[1], James W. Baish[8], Lance L. Munn[1], Jessalyn M. Ubellacker[9], Dennis Jones[6], Timothy P. Padera[1*]

[1]Edwin L. Steele Laboratories, Department of Radiation Oncology, Massachusetts General Hospital Cancer Center, Massachusetts General Hospital and Harvard Medical School, Boston, MA 02114, USA.

[2]Department of Anesthesia, Critical Care and Pain Medicine, Massachusetts General Hospital, Boston, MA 02114, USA.

[3]Corrigan-Minehan Heart Center and Cardiology Division, Massachusetts General Hospital, Harvard Medical School, Boston, MA 02114, USA.

[4]University at Buffalo Jacobs School of Medicine and Biomedical Sciences, Buffalo, NY 14203, USA.

[5]Harvard–MIT Division of Health Sciences and Technology, Massachusetts Institute of Technology, Cambridge, MA 02139, USA.

[6]Department of Pathology and Laboratory Medicine, Boston University Chobanian & Avedisian School of Medicine, 670 Albany Street, Boston, MA 02118, USA.

[7]Koch Institute for Integrative Cancer Research, Massachusetts Institute of Technology, Cambridge, MA 02142, USA.

[8]Department of Biomedical Engineering, Bucknell University, Lewisburg, PA 17837, USA.

[9]Department of Molecular Metabolism, Harvard T.H. Chan School of Public Health, Boston, MA 02115, USA.

[#]Equal contribution

*Corresponding author

Contact: tpadera@mgh.harvard.edu

Abstract

Lymphatic muscle cells (LMCs) within the wall of collecting lymphatic vessels exhibit tonic and autonomous phasic contractions, which drive active lymph transport to maintain tissue-fluid homeostasis and support immune surveillance. Damage to LMCs disrupts lymphatic function and is related to various diseases. Despite their importance, knowledge of the transcriptional signatures in LMCs and how they relate to lymphatic function in normal and disease contexts is largely missing. We have generated a comprehensive transcriptional single-cell atlas—including LMCs—of collecting lymphatic vessels in mouse dermis at various ages. We identified genes that distinguish LMCs from other types of muscle cells, characterized the phenotypical and transcriptomic changes in LMCs in aged vessels, and uncovered a pro-inflammatory microenvironment that suppresses the contractile apparatus in advanced-aged LMCs. Our findings provide a valuable resource to accelerate future research for the identification of potential drug targets on LMCs to preserve lymphatic vessel function as well as supporting studies to identify genetic causes of primary

lymphedema currently with unknown molecular explanation.

Keywords: Lymphatic muscle cells, single-cell RNA sequencing, lymphatic pumping, lymphatic contraction, ion channel, aging

Running title: Single-cell Transcriptional Atlas of Murine Lymphatic Muscle Cells

Introduction

The lymphatic vascular system plays a crucial role in maintaining tissue-fluid balance, absorbing dietary lipids, and transporting antigens and immune cells to lymph nodes (Petrova and Koh, 2018). Lymph—which is composed of absorbed interstitial fluid, macromolecules and immune cells—is formed by initial lymphatic vessels and drained into collecting lymphatic vessels, which transport the lymph to lymph nodes and eventually back to the bloodstream (Alitalo, 2011; Mäkinen et al., 2021; Oliver et al., 2020; Petrova and Koh, 2018, 2020). Initial lymphatic vessels are composed of a single layer of oak-leaf shaped lymphatic endothelial cells (LECs) sitting on a fenestrated basement membrane with button-like junctions between LECs (Baluk et al., 2007; Breslin et al., 2019). These button-like junctions allow for the collection of interstitial fluid and macromolecules to form lymph (Trzewik et al., 2001). Muscle cells are absent in the wall of initial lymphatic vessels (Baluk et al., 2007; Mäkinen et al., 2021). In contrast, the wall of collecting lymphatic vessels has three layers: an inner layer of endothelium, a middle layer of muscle cells responsible for autonomous phasic contractions, and an outer layer of fibroblasts and a collagen-enriched matrix that connects the vessels to surrounding tissues (Breslin et al., 2019; Bridenbaugh et al., 2013; Petrova and Koh, 2020). In addition, the collecting lymphatic vessels also contain intraluminal valves that prevent backflow and enable unidirectional propulsion of the lymph (Breslin et al., 2019; Zawieja, 2009). Until recently, LMCs were not recognized as a cell type distinct from vascular smooth muscle cells (VSMCs) (Kenney et al., 2020; Muthuchamy et al., 2003). Our data presented here directly show that LMCs are a unique cell type, distinct from other muscle cells including VSMCs.

Dysfunction of the lymphatic system is attributed as the cause of lymphedema and lymphatic diseases, which affect an estimated 7 million patients in the US and 250 million patients worldwide (Rockson, 2018, 2021). Further, there are strong associations for the involvement of the lymphatic system in the pathogenesis of many diseases, including bacterial and filarial infections (Jones et al., 2018; Zhou et al., 2019), inflammatory bowel disease (Rehal et al., 2018), metabolic syndrome (Jiang et al., 2019; Lee et al., 2022; Norden and Kume, 2020), congestive heart failure (Itkin et al., 2021), hypertension (Chachaj et al., 2018), diabetes (Cao et al., 2021) and neurodegenerative diseases (Louveau et al., 2018), including Alzheimer's disease (Da Mesquita et al., 2018). Further, the recovery from many pathologies, including myocardial infarction (Klaourakis et al., 2021; Liu et al., 2020) and bone regeneration (Biswas et al., 2023), also requires the lymphatic system. Altering the growth and function of the lymphatic system in these diseases and repair processes is a promising therapeutic strategy. Incredibly, there are currently no FDA approved drugs indicated to alter lymphatic function. The discovery of lymphatic vessel-specific therapeutics requires a deep characterization of lymphatic biology that is only now emerging. In the late 1990s and early 2000s, the identification of vascular endothelial growth factor receptor 3 (VEGFR-3) (Kaipainen et al., 1995; Kukk et al., 1996), prospero homeobox 1 (PROX1) transcription factor (Hong et al., 2002; Petrova et al., 2002; Wigle and Oliver, 1999; Wigle et al., 2002), integral membrane glycoprotein podoplanin (PDPN) (Wetterwald et al., 1996), and lymphatic vessel endothelial hyaluronan receptor 1 (LYVE1) (Banerji et al., 1999; Jackson et al., 2001) as critical molecular regulators of LECs revolutionized the field of lymphatic biology research. However, the study of LMCs has fallen

behind LECs, in part due to the lack of a comprehensive characterization of LMCs (Kenney et al., 2020). Therefore, it is imperative to improve our knowledge of the molecular signaling in LMCs and their contributions to lymphatic function.

In addition to secondary lymphedemas, many lymphedema patients have congenital primary lymphedemas. Considerable research has not only been dedicated to identifying genes associated with primary lymphedemas to help with diagnosis and to understand the disease pathogenesis, but also to build our understanding of the critical signaling pathways involved in the formation, growth, maturation and function of lymphatic vessels (Brouillard et al., 2021; Mäkinen et al., 2021; Martin-Almedina et al., 2021; Witte et al., 2021). Even with these focused efforts, many cases of primary lymphedema do not have an identified mechanism yet. It is likely that dysfunction of LMC activity and lymphatic contraction are the root cause of lymphedema in some of these patients, as is the case for patients with Cantú syndrome (Davis et al., 2023). The lack of a molecular characterization of LMCs hinders the ability to assign the molecular cause of these primary lymphedemas as well as impairs the ability to discover critical signaling mechanisms necessary for maintaining contractile activity of lymphatic vessel.

Damage to LMCs causes lymphatic pump failure leading to edema and locally immunocompromised tissues (Muthuchamy et al., 2003; Padera et al., 2016; Scallan et al., 2016; Zawieja, 2009). We reported that impaired LMC contraction reduces antigen transportation and is associated with immunosuppression (Liao et al., 2011). Further, we showed that death of LMCs caused by bacterial infection can permanently stop lymphatic pumping (Jones et al., 2018). In addition, functional studies in aged mice and rats have shown decreased LMC coverage of the mesenteric lymphatics (Gashev, 2010), reduced muscle contraction (Akl et al., 2011; Nagai et al., 2011), decreased ion channel protein expression (Zolla et al., 2015), and decreased collecting lymphatic ejection fraction (Akl et al., 2011; Liao et al., 2011; Nagai et al., 2011). Aged mice have decreased lymphatic vessel density, increased lymphatic permeability, and decreased ability to clear bacteria (Kataru et al., 2022). The loss of the contractile phenotype in LMCs during aging causes the reduction of lymph pumping and drainage (Akl et al., 2011), which may help explain the increased infection rate and weakened response to pathogens and vaccines—including COVID-19 vaccines—in older adults (Bartleson et al., 2021).

Single-cell transcriptomics has enhanced our understanding of cell composition and gene expression in lymphatic vessels (Kenney et al., 2022) and lymph nodes (Fujimoto et al., 2020; Rodda et al., 2018; Takeda et al., 2019; Veerman et al., 2019). In this study, leveraging single-cell RNA-sequencing and intravital lymphangiography, we characterized the phenotypes and gene expression plasticity of LMCs in both male and female mice across the lifespan. Our study provides a comprehensive characterization of murine dermal collecting lymphatic vessels and their microenvironment, which will provide the fundamental knowledge to facilitate the study of LMCs in order to identify targets to preserve lymphatic vessel function. Further, identifying the distinct gene signatures of LMCs will provide novel strategies for visualization and cell lineage tracing in collecting lymphatic vessels. Finally, these data will help identify the origins of LMCs during development, the mechanisms driving the regeneration of lymphatic vessels, and the mechanisms involved in various pathophysiological processes, including the onset of primary lymphedema.

Results

The single-cell landscape of collecting lymphatic vessels from mouse dermis across lifespan

To characterize the transcriptomes of the cells that make up the walls of collecting lymphatic

vessels and the surrounding tissue, we isolated dermal collecting lymphatic vessels that connect the inguinal lymph node and axillary lymph node (**Figure S1**) in 6-week-old (young), 12-month-old (middle-aged), and 18-month-old (aged) C56BL/6J mice from both males and females for 10X Genomics single-cell library construction and subsequent Illumina high throughput sequencing. The total number of reads ranged from 75 million to 100 million in all the samples (**Table 1**). After rigorous quality control (see Methods), 31,140 single-cell transcriptomes passed the quality threshold for downstream analysis. Specifically, we obtained 15,755 single cells in the young group, 5,503 in the middle-aged group, and 9,882 in the aged group (**Table 1**). Of note, the number of cells obtained from male and female mice is comparable, with 14,631 single cells from male mice and 16,509 from female mice (**Table 1**). The average number of genes per cell is between 1000 to 2000 in all samples, and the percentage of mitochondrial genes was less than 5% (**Table 1**), demonstrating the high quality of our single-cell RNAseq datasets (Luecken and Theis, 2019).

Uniform manifold approximation and projection (UMAP) analysis of all the single cells grouped them into 13 cell clusters (Stuart et al., 2019) (**Figure 1A**). Cell type annotations were guided by known marker gene expression (Cohen et al., 2018; Han et al., 2018; Jones et al., 2018; Kalucka et al., 2020; Muhl et al., 2020; Muthuchamy et al., 2003; Petrova and Koh, 2018; Renner et al., 2017; Russell et al., 2022; Siret et al., 2022) (**Figure 1B**) and annotated by age and sex of the mouse of origin (**Figure 1C** and **Table 2**). Our data include a population of *Acta2* and *Notch3* expressing cells that we determined to be LMCs. The presence of large amounts of mesenchymal/fibroblasts, macrophages and epithelial cells in our single-cell data suggests that they are positioned close to the lymphatic vessels and may play a previously unrecognized role in regulating lymphatic vessel function. This is supported by recent data that reported infiltration of tissue-resident macrophages contributes to lymphatic vessel regeneration after injury (Razavi et al., 2023). The CD34+ endothelial cells are likely from adjacent capillaries (Breslin et al., 2019).

Myoepithelial cells also express the common smooth muscle cell genes *Acta2* and *Tagln*, (**Figure S2A**), but other common marker genes expressed in smooth muscle cells, including *Mustn1*, *Notch3*, *Des*, and *Rgs4* were absent in myoepithelial cells. In addition, *Krt5*, *Krt14*, *Krt17*, and *Cxcl4* were expressed in the myoepithelial cell cluster but not in LMCs (**Figure S2A**). Previous research has reported that myoepithelial cells express *Krt5*, *Krt14*, *Krt17*, and *Cxcl4*, as well as mild levels of *Acta2* and *Tagln* (Han et al., 2018; Kanaya et al., 2019; Karaayvaz et al., 2018), supporting our findings. Of note, 92% of the myoepithelial cells are from female mice (**Figure 1C** and **Table 2**), indicating they are likely to arise from adjacent mammary glands, which are anatomically close to the dermal collecting lymphatic vessels in mice. To confirm this hypothesis, we combined the myoepithelial cells and LMCs from our data with a published single-cell RNA sequencing dataset from murine mammary fat pads (Li et al., 2020). Our analysis showed that LMCs clustered with pericytes, whereas the myoepithelial cells in our dataset clustered with myoepithelial cells in the mammary fat pad dataset (**Figure S2B**).

Overall, we have generated a comprehensive single-cell transcriptomic atlas of murine collecting lymphatic vessels and the adjacent tissues across the lifespan.

Characterization of the LMC-specific gene signature

Currently, the most commonly employed markers to identify LMCs are αSMA (encoded by *Acta2*) (Jones et al., 2018; Kenney et al., 2020; Russell et al., 2022) and *Myh11* (Muthuchamy et al., 2003). However, these two markers are general markers for smooth muscle cells including VSMCs. Several studies have demonstrated a rich diversity of smooth muscle cells (Liu et al., 2019; Muhl et

al., 2022). In addition, it is well-recognized that the LMCs display distinct phenotypes and functions not seen in VSMCs, such as autonomous phasic contractions (Scallan et al., 2016). To identify the unique markers for LMCs, we integrated the LMCs single-cell RNA sequencing data with several seminal studies of muscle cells from different organs, including skeletal muscle cells (GSE143437) (De Micheli et al., 2020), cardiomyocytes (GSE95140, GSE132658, GSE153481) (Goodyer et al., 2022; Nomura et al., 2018; Wang et al., 2020), and vascular smooth muscle cells (GSE203594) (Xu et al., 2022) (**Figure 2A**). We identified a group of genes that are predominantly expressed in LMCs (**Figure 2B**), including *Thbs1*, *Nr4a2*, *Nr4a3*, *Scn3a*, *Adamts4* and *Kcne4*. Of note, *Notch3* has been shown to be a unique marker gene for smooth muscle cells in the heart, lung, and colon, but not in the aorta (Muhl et al., 2022). We also found that LMCs expressed *Notch3* in our single-cell data (**Figure S2A**) and confirmed the presence of Notch3 in LMCs by whole mount immunofluorescence staining (**Figure S3A**). Myosins and actin filaments are the essential components of the muscle cell contractile apparatus (Sweeney and Hammers, 2018). Examination of the single-cell gene expression identified distinct myosins (**Figure 2C-D**) and actin filament molecules (**Figure 2E**) that were expressed in different muscle cells. We found LMCs expressed myosins and actin filaments that are largely similar to aortic smooth muscle cells, including myosin light chain molecules *Mylk*, *Myl9*, *Myl6* (**Figure 2C**), myosin heavy chain molecules *Myh11* and *Myh9* (**Figure 2D**), and actin filament molecules *Actg1, Actb,* and *Acta2* (**Figure 2E**). Cardiomyocytes and skeletal muscle cells showed different expression patterns of actin and myosin molecules (**Figure 2C-E**).

Differential expression of ion channels in LMCs

Generating electrical action potentials in LMCs creates spontaneous contractions (Hald et al., 2018). Ion channels are necessary to generate action potentials by modulating membrane potential and intracellular calcium concentration (Tykocki et al., 2017). Among these channels, voltage-gated calcium channels (VGCC), voltage-gated potassium (KV) channels, and Ca2+-activated potassium (BK) channels are considered key regulators of vascular smooth muscle excitability and contractility (Pereira da Silva et al., 2022). To examine the presence of ion channels in LMCs, we investigated the expression of calcium, chloride, potassium and sodium channel molecules across different muscle cells.

<u>Calcium channels:</u>

In contrast to myosin expression where LMCs share similarities with VSMCs, calcium channel expression in LMCs resembled that of cardiomyocytes (**Figure 3A**), including T-type calcium channel genes *Cacna1g* and *Cacna1h* ($Ca_V3.1$ and $Ca_V3.2$, respectively), and L-type calcium channel genes *Cacna1c* ($Ca_V1.2$) (Lee et al., 2014). While L-type calcium channels contribute to the upstroke of the LMC action potential (Telinius et al., 2014a), a recent study showed that T-type calcium channels likely play a minimal or no role in lymphatic pacemaking in mice, despite being present in LMCs (To et al., 2020). Leveraging our intravital lymphatic contraction assay (**Figure S4A**) (Jones et al., 2018; Liao et al., 2011, 2014), we evaluated the effect of calcium channel blockers on lymphatic contraction. We tested the L-type calcium channel blocker (nifedipine) (Lee et al., 2014) and T-type calcium channel blocker (mibefradil) (Lee et al., 2014; To et al., 2020). Of note, at high concentrations, mibefradil can also block L-type calcium channels (Leuranguer et al., 2001). The blockers were administrated either locally [8 μl of nifedipine (17 mg/ml in EtOH) or mibefradil (20 mg/ml)] or systemically [i.p., mibefradil (15 mg/kg)]. The strength of the lymphatic contraction was measured by the ejection fraction—theoretical fractional volume of lymph

expelled with each vessel contraction (Jones et al., 2018; Liao et al., 2011, 2014). We found that each of these calcium channel inhibitors can reduce lymphatic contraction after both local and systemic injections (**Figure 3B**). Mibefradil was able to maintain a reduced ejection fraction and contraction frequency for at least 6 hours (**Figure S4B**). These data are consistent with published data in isolated collecting lymphatic vessels (Lee et al., 2014; Telinius et al., 2014a; To et al., 2020), highlighting the importance of calcium channels in lymphatic contractility (Davis et al., 2023b; Russell et al., 2022).

The release of calcium from the sarcoplasmic reticulum in muscle cells is mediated by ryanodine receptors (RyR) (Felder et al., 2002). Previous studies have reported the presence of RyR in lymphatic vessels and showed that doxorubicin can activate RyR in rat LMCs, causing calcium leak to suppress lymphatic contraction and cause lymphostasis (Stolarz et al., 2019). Dantrolene, a RyR antagonist, prevented doxorubicin-mediated lymphostasis (Van et al., 2021). In line with previous research, we found modest expression of the gene encoding the ryanodine receptor *RyR2* in a small subset of mouse LMCs (**Figure S5A**), consistent with the findings reported in collecting LMCs in rats (Jo et al., 2019).

Chloride Channels:

The calcium-activated chloride channel, anoctamin-1 (ANO1, gene *Ano1*), also called TMEM16A, contributes to the diastolic depolarization of LMCs and partially sets the lymphatic contraction rate (Zawieja et al., 2019). Consistent with these established findings, we found the presence of *Ano1* mRNA in our murine LMC dataset (**Figure 3C**). Similar to aortic smooth muscle cells, we also find *Ano6* mRNA in LMCs (**Figure 3C**), which has not previously been described. While voltage-gated chloride channels have not previously been described in LMCs, our data show expression of *Clcn4* mRNA in LMCs, as well as in cardiac and aortic muscle cells (**Figure 3D**). Volume-regulated anion channels (VRACs) regulate cell size by passing chloride ions and osmolytes across the cell membrane and have been found to modulate the rate of spontaneous contractions of lymphatic vessels (Solari et al., 2023), but the specific subunits involved are undefined. The genes for the VRAC subunits *Lrrc8a* and *Lrrc8c* are present in our LMC dataset (**Figure S5B**). It is worth noting that the ligand-gated chloride channels were absent in our murine LMC dataset. Similar to cardiac and aortic myocytes, we found LMCs express *Clic1* and *Clic4*—members of the chloride intracellular channel protein family (**Figure S5C**), which has not been previously described in LMCs.

Potassium channels:

Studies in sheep showed LMC membrane depolarization with exposure to 4-aminopyridine (4-AP), a broadly acting voltage-gated potassium channel inhibitor (Beckett et al., 2007). A previous study showed that the mRNA for the specific *KCNA2* isoform (gene for Kv1.2, a 4-AP sensitive channel) was present in human thoracic duct (Telinius et al., 2014b). In our dataset, we confirm the presence of *Kcna2* mRNA in LMCs and observe some LMCs expressing mRNA for *Kcna5* (protein Kv1.5, critical in atrial myocytes), and *Kcnb1* (protein Kv2.1) (**Figure 3E**). Kv7.4 channels (*Kcnq4*) are not blocked by 4-AP and play a crucial role in the hair cells of the inner ear by participating in potassium recycling, with mutations leading to deafness. Kv7.4 is also found in aortic smooth muscle and in a subset of LMCs in our dataset (**Figure 3E**), which has not been previously described in LMCs.

A *KCNK3* single-nucleotide polymorphism (SNP) was associated with development of secondary lymphedema following breast cancer surgery (Smoot et al., 2017), but neither *Kcnk3* nor any other

two-pore domain potassium channels have yet been demonstrated in LMCs (Lee et al., 2022). Our data show *Kcnk3* expression (protein K2P3, also called TASK) in LMCs (**Figure 3F**).

LMCs are known to express *Kcnj8* (ATP sensitive potassium channel Kir6.1) across multiple species and *Kcnj11* (protein Kir6.2) is expressed in some LMC populations (Davis et al., 2022). Cantú syndrome, which has a lymphedema phenotype, can be caused by mutations in the genes *Kcnj8* or *ABCC9* (Davis et al., 2023a). We observed the expression of *Kcnj8*, *Kcnj11*, *Abcc8*, and *Abcc9* genes in a small subset of LMCs (**Figure S5D**). Ether-a-go-go related gene (ERG) potassium channels are key in the repolarization phase of the LMC action potential, and ERG1 (encoded by *KCNH2*) was found to be present in LMCs of multiple species (Kim et al., 2023). We did not find significant mRNA for *Kcnh2* in murine LMCs in our dataset (**Figure S5E**).

Sodium channels:
Voltage-gated sodium currents were first found in sheep lymphatic muscle (Hollywood et al., 1997). Consistent with a published report in human thoracic duct (Telinius et al., 2015), we found that *Scn3a*, which encodes the sodium channel $Na_V1.3$, is highly expressed in LMCs (**Figure 3G**), Of note, not all the LMCs expressed *Scn3a* (**Figure 3G**), suggesting heterogeneity in the LMC population.

Hyperpolarization-activated cyclic nucleotide-gated (HCN) channels:
The role of HCN channels in lymphatic pacemaking is controversial (McCloskey et al., 1999; Negrini et al., 2016). Studies have demonstrated that they might play a role in human collecting vessels (Majgaard et al., 2022). We did not find strong mRNA expression of HCN genes in LMCs (**Figure S5F**).

Connexins:
Connexins have been studied in lymphatic vessels, especially in LECs (Meens et al., 2014). Connexin 37 is required for mouse lymphatic valvulogenesis and development of the thoracic duct (Kanady et al., 2011). In breast cancer patients, mutations in connexin genes correlate with secondary lymphedema following surgery (Hadizadeh et al., 2018). In LMCs, Connexin 45 (gene *Gjc1*) was identified as the critical connexin mediating pacemaker signaling conduction and entrained contractions, with deletions leading to 10-18 fold decrease in conduction speed (Castorena-Gonzalez et al., 2018). We identified the presence of mRNA for *Gja4* (protein: Connexin 37) and *Gjc1* (protein: Connexin 45) in LMCs (**Figure 3H**), confirming existing knowledge about Connexin 45 and suggesting that Connexin 37 may also play a role in LMCs, not just in LECs.

Through the use of freshly isolated collecting lymphatic vessels, our transcriptomic profile of LMCs is consistent with published literature, providing validation of our dataset. Collectively, the LMC transcriptional profile aligns with their phenotypic properties. LMCs can maintain vessel tone similar to VSMCs, yet they can also generate action potential-driven contractions analogous to cardiomyocytes. The distinctive transcriptional activity of LMCs demonstrates similarities to both of these cell types, while distinguishing LMCs as a unique cell type.

LMC transcription as a function of biological sex

Primary lymphedema is a well-recognized sex-linked disease, with a prevalence that is approximately three times higher in females than in males (Morfoisse et al., 2018, 2021; Smeltzer et al., 1985; Vignes et al., 2021). However, the impact of biological sex on LMC in lymphedema is still poorly understood. We compared the gene expression profiles of LMC between male and female mice and identified 267 differentially expressed genes (**Figure S6A-B**). To gain further insight

into the biological consequences of these differentially expressed genes, we performed signaling pathway analysis using PROGENy. Our results showed that estrogen, Trail, MAPK, JAK-STAT, and WNT signaling pathways were up-regulated in the LMC of female mice. In contrast, TGFβ, PI3K, p53, EGFR, TNFα, and NFκB signaling pathways were elevated in the LMC of male mice (**Figure S6C**).

Lymphatic contraction is impaired and LMC coverage reduced in aged mice

The reduction of mesenteric lymphatic contraction has previously been reported in aged rats (Akl et al., 2011; Nagai et al., 2011) and in peripheral collecting lymphatic vessels in mice (Liao et al., 2011), which is attributed to a reduction of LMC coverage (Gashev, 2010). To examine the impact of aging on lymphatic function, we measured the collecting lymphatic vessel pumping frequency and intensity in young and aged C57BL/6J mice with the intravital fluorescent microscopy (Jones et al., 2018; Liao et al., 2011, 2014). Compared to young mice, the lymphatic vessel contraction strength and frequency in the aged group was significantly decreased (**Figure 4A-B**). Whole mount immunofluorescence staining for αSMA shows that the density of LMCs in aged mice declined substantially (**Figure 4C**). Further, LMCs in the young mice displayed a more circumferential orientation around the vessels compared to LMCs in aged mice, which were more longitudinally oriented along the vessels (**Figure 4C**). The altered orientation of LMCs on the wall in aged lymphatic vessels likely affects their pumping capacity (Kataru et al., 2022).

LMCs transition from a contractile to synthetic phenotype during aging

To understand the transcriptomic alterations in LMCs during aging, we compared the differentially expressed genes between young and aged LMCs. We found 429 differentially expressed genes with a cutoff p-value < 0.05 and fold-change > 0.5 (**Figure 5A**). Gene Set Enrichment Analysis (GSEA) analysis indicates that RNA processing-related gene signatures were up-regulated in the aged LMCs, while supramolecular fiber organization, actin filament-based process, muscle system process, and ion transmembrane transport-related gene signatures were down-regulated in aged LMCs (**Figure 5B**). In addition, we also found that muscle cell contractile apparatus-associated molecules were significantly down-regulated in aged LMCs, including *Acta2*, *Myh11*, *Tpm2*, *Lmod1*, *Col4a1*, *Lamb2*, *Col1a2*, *Col3a1*, *Eln*, and *Col1a1* (**Figure 5C**). The down-regulation of *Acta2* and *Myh11* gene-expression in aged lymphatic vessels was further confirmed by real-time PCR (**Figure 5D**). VSMCs have been shown to be heterogenous, with some displaying a contractile phenotype (enhanced expression of *Acta2*, *Myh11*, *Tagln*, *Myocd*, and *Smtn*) and others displaying a synthetic phenotype (enhanced expression of *Klf4*, *Rbp1*, and *Mmp2*) (Rensen et al., 2007). Our data suggest a similar contractile to synthetic transition occurs in LMCs during aging as shown by the down regulation of contractile associated genes in aged LMCs.

TNFα can drive the contractile to synthetic switch of LMCs in aged lymphatic vessels

Previous studies suggest that the cells in lymphatic vessel adjacent tissue impact the contraction of LMCs by releasing signaling molecules, such as nitric oxide (Chen et al., 2017; Liao et al., 2011; Rehal et al., 2020). To understand whether the transition of the LMC phenotype from contractile to synthetic during aging was attributed to paracrine signals from the adjacent tissue, we analyzed cell-cell interactions of each signaling pathway in the single cell RNA sequencing datasets from young and aged lymphatic vessels to identify the conserved and context-dependent signaling pathways. We found that MK, NCAM, GRN, CD200, CD23, IL4, and MPZ cell-cell communication probabilities were greater in the lymphatic vessels in young mice (**Figure S7A)**. In contrast, the

TGFβ, ANNEXIN, ITGAL-ITGB2, FGF, IL6, BMP, EPHB, NECTIN, WNT, NRXN, EPHA, GDF, VISFATIN, and TNF cell-cell communication probabilities were significantly enriched in the aged lymphatic vessels (**Figure S7A**). To examine whether these signals were directly targeting LMCs, we performed ligand-receptor communication probability analysis (Jin et al., 2021). We found that Tnf-Tnfrsf1a, Igf-Igf1r, Fgf2-Fgfr1, and Bmp2-(Bmpr1a+Bmpr2) ligand-receptor interactions were significantly up-regulated in aged LMCs (**Figure 6A**). The cell-cell interaction network analysis of the TNF signaling pathway indicated Lyve1+ macrophages, S1008a+ S100a9+ macrophages and mast cells were the major cell types that frequently interact with LMCs in aged mice (**Figure 6B**). Single-cell gene expression analysis also showed a high level of *Tnf* mRNA in Lyve1+ macrophages, S1008a+ S100a9+ macrophages and mast cells in aged mice (**Figure 6C**). To test if TNFα can induce a contractile to synthetic transition in LMCs, we isolated LMCs from young mice and cultured the LMCs *in vitro* in the presence or absence of TNFα (10 ng/mL) (Arroyo-Ataz and Jones, 2022). We found that TNFα suppressed the gene expression of *Myh11* and *Acta2* (**Figure 6D**). Taken together, we hypothesize that in aged lymphatic vessels, TNF-α derived from macrophages and mast cells suppresses the contractile apparatus in LMCs, resulting in a reduction of lymphatic contraction (**Figure 6E**).

Discussion

With hundreds of millions of patients around the globe suffering from lymphedema and lymphatic diseases (Rockson, 2018, 2021), our therapeutic tools to help these patients are severely lacking, making these patients some of the most underserved by biomedical research. The lymphatic system covers the surface of the brain (Louveau et al., 2015) and is in the tips of the toes and is in every organ system in between, yet there are no FDA approved drugs indicated to alter its function. One limitation is the lack of fundamental knowledge of molecular phenotypes of all the cell types necessary to build and drive the function of lymphatic vessels. Rapid progress has been made in characterizing the critical lymphatic endothelial cell (Alitalo, 2011; Aspelund et al., 2016; Baluk et al., 2007; Ducoli and Detmar, 2021; Hong et al., 2002; Oliver et al., 2020; Takeda et al., 2019; Wigle et al., 2002), but limited recognition of LMCs as a unique cell type, distinct from VSMCs, has hindered progress. Due to their important functional roles in driving lymph flow, LMCs are important targets for potential therapeutics. Here, we provide a comprehensive characterization of the LMC transcriptomic output across the lifespan, accounting for biological sex (**Figure 1A&C**). Our data directly show that LMCs are a unique muscle cell type with similarities in transcriptional activity to some aspects of both VSMCs and cardiomyocytes (**Figure 2C-E and Figure 3A**), consistent with the functional activity of LMCs in driving lymphatic pumping (Scallan et al., 2016; Zawieja, 2009). This dataset provides a resource that can spur discovery of targeted therapeutics to alter lymphatic vessel contractility by altering activity of LMCs or restoring lost LMC activity that occurs with aging. Further, this data resource can be used to help link genetic mutations associated with human primary lymphedemas to testable functional consequences for the lymphatic system. Through newly uncovered connections in primary lymphedema, further discovery of fundamental lymphatic biology can occur as well as the potential to develop therapies for patients suffering from these primary lymphedemas.

Through single-cell RNA sequencing analysis, we uncovered a list of LMC marker genes (**Figure 2B**), including *Thbs1*, *Nr4a2*, *Nr4a3*, *Scn3a*, *Adamts4* and *Kcne4*. In addition, we discovered that LMCs express myosin heavy and light chain as well as actin filament molecules similarly to VSMC (**Figure 2C-E**). This is supported by a recent study that utilized Cre-tdTomato reporter mice specific for progenitors of skeletal muscle cells ($Pax7^+$ and $MyoD^+$) and VSMCs ($Prrx1^+$ and

NG2$^+$) to investigate the origin of LMCs in lymphatic vessels afferent to the popliteal lymph node (PLV-LMCs) (Kenney et al., 2020, 2023). The study demonstrated that PLV-LMCs originate from Pax7$^-$/MyoD$^-$/Prrx1$^+$/NG2$^+$ progenitors—similarly to VSMCs—prior to postnatal day 10. However, after postnatal day 10, PLV-LMCs originate from a previously unknown Pax7$^-$/MyoD$^-$/Prrx1$^+$/NG2$^-$ muscle progenitor.

Voltage-gated calcium channels transduce membrane depolarization into augmented Ca2+ influx into cells and play an important role in the regulation of both contraction and gene expression in vascular smooth muscle cells (Pereira da Silva et al., 2022; Tykocki et al., 2017), cardiomyocytes (Marbán, 2002), and LMCs (Lee et al., 2014; To et al., 2020). The intracellular calcium channel serves as a phase controller by regulating the myosin-light-chain kinase activity (Kim et al., 2008). Depolarization of LMCs activates and opens L-type voltage-gated calcium channels and mediates entry of Ca2+ into LMCs, which is crucial for excitation-contraction coupling (Lee et al., 2014; To et al., 2020). As expected, we found both L-type and T-type voltage gated calcium channels in LMCs (**Figure 3A**). In addition, our functional data confirms that the calcium channel blockers nifedipine and mibefradil decrease lymphatic contraction frequency and strength (**Figure 3B**). Ryanodine receptors in the sarcoplasmic reticulum also contribute to calcium release and electromechanical coupling (Stolarz et al., 2019; Van et al., 2021). Our findings indicate that LMCs express RyR2 (**Figure S5A**), suggesting a potential unrecognized role in regulating lymphatic contraction.

The voltage-gated sodium channel, Nav1.5, is crucial for generation of the cardiac action potential, and vascular smooth muscles lack voltage-gated sodium channels. Previous studies indicate that the contribution of voltage-gated sodium channels to the lymphatic action potential may vary by species (Chan and von der Weid, 2003; Ohhashi et al., 1980; Telinius et al., 2015). Tetrodotoxin, a blocker of several types of voltage-gated sodium channel sensitive currents are found in human (Telinius et al., 2015) and sheep, but not in bovine (Ohhashi et al., 1980) or guinea-pig (Chan and von der Weid, 2003) lymphatic vessels. We find that Nav1.3 mRNA is present in murine LMCs (**Figure 3G**).

In addition to voltage-gated sodium channels, multiple other channel types, such as Ano1, HCN, and other cationic channels may contribute to the pacemaking and upstroke of lymphatic depolarization. Different from rat (Negrini et al., 2016), sheep (McCloskey et al., 1999) and human (Majgaard et al., 2022) lymphatic vessels—which have HCN-mediated currents—the mRNA expression for HCN was minimal in our murine LMC dataset (**Figure S5F**). *Ano1* was present in our dataset (**Figure 3C**), consistent with its known role in LMC depolarization (Zawieja et al., 2019). Additionally, the transcript for another calcium-activated chloride channel, *Ano6*, was also present (**Figure 3C**), although it has not been previously studied in LMCs. We also identified that LMCs expressed chloride channel genes *Clic1* and *Clic4* (**Figure S5C**), which have not been studied in LMCs. After depolarization and initiation of LMC twitch contraction, the cells must repolarize to reset the resting membrane potential. In cardiomyocytes, repolarization is driven by a multitude of potassium channels (Grant, 2009), and the same has been presumed for LMCs (Kim et al., 2023). Consistent with existing LMC literature, we found the following potassium channel genes: *Kcna2* (Kv1.2), *Kcnj8* (Kir6.1), *Kcnj11* (Kir6.2), *Abcc9* (SUR2), *Kcnh2* (ERG1) (**Figure 3E, S5D-E**). Additional transcripts for potassium channels identified by our dataset which have not previously been studied in LMCs includes: *Kcna5* (protein Kv1.5), *Kcnb1* (Kv2.1), *Kcnq4* (Kv7.4), *Kcnk3* (K2P3), and *Abcc8* (SUR1) (**Figure 3E-F, S5D**). In addition, the voltage-gated potassium (Kv) channel β subunit gene *Kcne4*, is expressed in LMCs, but not in cardiomyocytes, skeletal muscle

or VSMCs (**Figure 2B)**. KCNE4 is known to inhibit the current of Kv2.1 and Kv7.4 (David et al., 2015), both of which are expressed on LMCs (**Figure 3E**). Electrically driven contraction mediated by LMCs needs to be propagated along a lymphangion for coordinated systole in a lymphatic vessel. The gap junction protein connexin 45 is involved in primary lymphedema, has been found to mediate entrainment of LMC contraction waves (Castorena-Gonzalez et al., 2018), and is also present in our dataset (*Gjc1*) (**Figure 3H**). In addition, we also identified the presence of *Gja4* (connexin 37) in LMCs (**Figure 3H**).

Aging is a natural process that affects all tissues and organs, including lymphatic vessels. As the body ages, oxidative stress can accumulate in lymphatic vessels (Thangaswamy et al., 2012). Mechanistically, the accumulation of reactive oxygen species and pro-inflammatory cytokines—such as tumor necrosis factor-alpha (TNFα), interleukin-1beta (IL-1β), interleukin-6 (IL6)—can promote the activation of "sheddases", including metalloproteinases, heparinase, and hyaluronidase (González-Loyola and Petrova, 2021). This pro-inflammatory microenvironment triggers the accumulation of sheddases and accelerates glycocalyx degradation, leading to vascular hyperpermeability, unregulated vasodilation, microvessel thrombosis, and increased leukocyte adhesion (González-Loyola and Petrova, 2021). Previous studies demonstrated that aging increases the proliferation and migration of VSMCs and accelerates the contractile to synthetic transition of these cells (Bochaton-Piallat et al., 2001; Rensen et al., 2007). Similarly, we also found the reduction of gene-expression of contractile-related genes in aged LMCs, which can be driven by the inflammatory cytokine TNFα that increases in tissues with age. Consequently, the phenotypic change of LMCs led to the attenuation of lymphatic pumping and drainage (**Figure 4A-B**). Further, the loss of muscle cells in lymphatic vessels can lead to a decrease in contraction frequency, systolic lymph flow velocity, and pumping activity, ultimately impairing lymph flow (Jones et al., 2018; Zolla et al., 2015). Consequently, age-related lymphatic impairment can cause various disorders, including imbalances in interstitial fluid homeostasis, abnormal lipid accumulation, and impaired immune responses to infections, cancers, and vaccines.

LMC-disruption has been linked to pathological conditions such as lymphedema (Scallan et al., 2016), which is characterized by swelling due to inadequate tissue interstitial fluid absorption and lymph transport. Lymphedema profoundly impacts a patient's life by limiting limb or organ function and making the patient prone to infections that often require hospitalization. Unfortunately, current treatments are cumbersome and often inadequate (Rockson, 2018, 2021). There is no cure for lymphedema. Our preclinical animal models have demonstrated that methicillin-resistant *Staphylococcus aureus* (MRSA), bacteria that often causes skin and soft tissue infections, can damage LMCs and stop lymphatic pumping and lymph flow (Jones et al., 2018). Persistent MRSA infections can progress to sepsis and individuals aged 65 years and older are particularly susceptible to sepsis (Lee et al., 2018; Moreira et al., 2021). Of note, the deficits in LMC coverage of lymphatic vessels persists even after the infection resolves, leading to questions of why LMC do not functionally regenerate (Jones et al., 2018). Determining the origin of LMCs and their developmental signaling will provide new strategies to regenerate LMCs on damaged lymphatic vessels. While the origins of LECs have been widely studied (Butler et al., 2009; Grimm et al., 2023; Gutierrez-Miranda and Yaniv, 2020; Hong et al., 2002; Petrova et al., 2002; Wigle and Oliver, 1999; Wigle et al., 2002), the origin and development of LMC remain largely unknown. In addition, whether or not LMC stem cells exist in adults remains an open question in the field.

A recent study has identified markers of cellular heterogeneity in subsets of smooth muscle cells across multiple organs (Muhl et al., 2022). In another study, Kenney et al. characterized the muscle

cells in popliteal lymphatic vessels in wild-type, Cspg4-Cre/Ai9-tdTomato, and TNF-Tg mice using fluorescence-activated cell sorting (FACS) for single-cell RNA sequencing (Kenney et al., 2022). In both studies, the cells were sorted with flow cytometry before single-cell RNA sequencing, which is known to alter the transcriptome of cells. In contrast, we generated droplet-based single-cell RNA sequencing profiles from all the cells in freshly isolated lymphatic vessels and adjacent tissues without presorting (**Figure 1A**). Our unbiased approach also allows the analysis of cell types previously lost to cell sorting. As we have shown in our data, *Acta2* and *Tagln* are also expressed in myoepithelial cells (**Figure 1B, S2A**), suggesting that the previous cell sorting-based approach could introduce bias to the datasets if they relied on αSMA to identify cells. Characterization of cell types with a few marker genes does not capture the spectrum of functional states and gene expression programs in lymphatic vessels. Our data show that by surveying all cells in the mouse dermal collecting lymphatic vessels, we identified markers of cellular heterogeneity and distinct cellular subpopulations that show plasticity with aging. In conclusion, we were able to utilize single-cell RNA sequencing to uncover the identity of LMCs and to analyze differential gene expression in LMCs across the murine lifetime (**Figure 5A-C**). Our findings provide markers of LMCs which will aid in their future study and may help associate gene mutations identified in patients with primary lymphedema with a functional deficit in their lymphatic system. In addition, we identified TNFα as a potential mechanism (**Figure 6A-D**) to help understand changes in lymphatic vessel function during aging.

The limitations of this study

In this study, we focused on the collecting lymphatic vessels in dermis, which often causes lymphedema in humans when damaged. It is possible that LMCs in mesenteric lymphatics and the thoracic duct may exhibit different gene signatures (Zawieja et al., 2018). Emerging data also suggest that lymphatic vessels exhibit organ-specific heterogeneity (Oliver et al., 2020; Petrova and Koh, 2018) and acquire distinct characteristics upon exposure to different tissue microenvironments (Aspelund et al., 2016; Biswas et al., 2023; Da Mesquita et al., 2018; Reed et al., 2019), which in turn enable them to execute multifaceted functions. Characterizing organ-specific lymphatic vessels and LMCs will help gain insight into their heterogeneity and specialization, enabling the specific targeting of organ-associated vessels for therapeutic purposes. In addition, our single-cell data is from mice and human LMCs may display different gene signatures.

Methods and materials

Mice

C57BL/6 mice were housed in animal facilities at Massachusetts General Hospital. Both male and female mice of ages 6 weeks, 12 months, and 18 months were utilized for this study. The 18-month-old mice were provided by the National Institute on Aging/National Institutes of Health. All animal procedures were subjected to review and approval by the Institutional Animal Care and Use Committees (IACUC) at Massachusetts General Hospital.

Collecting lymphatic vessel isolation

Mice were anesthetized with ketamine (100 mg/kg) and xylazine (10 mg/kg) via intraperitoneal injection. The ventral fur was removed via shaving and the surgical site was disinfected with 70% ethanol. A ventral midline skin incision was made from the pubis to the sternum. Lateral incisions were extended from the midline to the upper and lower limbs. The skin was then opened laterally to expose the collecting lymphatic vessels that connect the inguinal lymph node and axillary lymph

node (inguino-axillary lymphatic vessels). To enhance the visibility of the lymphatic vessels, 4 µL of Evans Blue (0.1% diluted in PBS) was injected into the inguinal lymph node and filled the lymphatic vessels from the inguinal to the axillary node. The collecting lymphatic vessels were isolated under a stereo microscope, and excess fat and connective tissues were removed while the vessels remained in situ within the mouse to maintain the health of the tissue during the surgical preparation of multiple mice. Once the vessels were cleaned from all mice, they were cut and removed from each mouse. The isolated lymphatic vessels were pooled and immediately transferred to a Petri dish containing high-glucose DMEM (Corning 10-013-CV) without FBS and kept on ice until digestion. Throughout the dissection, mice were kept under anesthesia to minimize pain and discomfort.

Single-cell RNA-Seq library preparation

Eight to ten mice were used in each of six groups (two sexes: male, female; and three ages: 6 weeks, 12 months, 18 months). The harvested lymphatic vessels were transferred into 1.5 mL Eppendorf tubes containing 1 mL of digestion buffer [10 mL high glucose Dulbecco's Modified Eagle Medium (DMEM) (Corning 10-013-CV) with 20 mg Collagenase I, 5 mg Elastase, 8 mg Dispase, and 1 mg DNaseI]. The vessels were incubated in a 37ºC swirling water bath for 40-60 minutes, with the digestion contents being gently resuspended every 5 minutes. After digestion, the samples were filtered through a 70 µM nylon mesh and quenched by adding fetal bovine serum (FBS) to a final concentration of 10%. The samples were then centrifuged at 300 rcf for 5 minutes at 4ºC. The supernatant was discarded, and the pelleted cells were resuspended in 1 mL of ACK lysis buffer and kept at room temperature for 2 minutes to remove the red blood cells. The ACK lysis reaction was quenched by adding 9 mL of FACS buffer (2% FBS + 1X DPBS). The resulting 10 mL sample was centrifuged at 300 rcf for 5 minutes at 4ºC. The pelleted cells were resuspended in 150-200 µL of FACS buffer and filtered through a 35 µM nylon cell strainer. Cell viability was confirmed by Trypan Blue (Gibco) staining through manual counting as well as TC20 automated cell counting (Bio-Rad). Only samples with > 74% live cells were processed with 10X Genomics Single Cell 3' Reagent Kit-based Gel Bead-In-Emulsions (GEM) reactions, followed by Illumina NextSeq 2000 sequencing with the High Output PE26/98 mode.

Single-cell RNA-Seq data analysis

The Cell Ranger analysis pipeline was utilized to pre-process and align raw fastq-format data and generate feature-barcode matrices (Zheng et al., 2017). Subsequently, Seurat was employed for graph-based single-cell clustering (Stuart et al., 2019). To ensure the selection of high-quality single-cell transcriptomic profiles, cells that had less than 100 genes or more than 10,000 featured RNAs detected or more than 25% mitochondrial genes, were excluded. Genes expressed in less than 3 cells were also removed. The R package SCpubr was used for single-cell RNA sequencing data visualization, pathway analysis, and transcription factor analysis (Blanco-Carmona, 2022). Cell cycle regression was performed based on the Seurat cell cycle scoring and regression method. Gene ontology functional annotation was performed using the ShinyGO software (Ge et al., 2020). Additionally, the CellChat R package (Jin et al., 2021) was used for cell-cell interaction network and ligand-receptor analysis, with the CellChatDB mouse database manually curated based on literature-supported ligand-receptor interactions. The R packages clusterProfiler (Wu et al., 2021) and msigdbr (Liberzon et al., 2015) were employed for Gene Set Enrichment Analysis.

RNA extraction and real-time PCR assay from lymphatic vessels

The collecting lymphatic vessels in 6-week-old and 18-month-old mice were isolated as described

above, and immediately placed in 1.5 mL Cryogenic vials (ThermoFisher Scientific) and kept in liquid nitrogen to preserve the RNA quality. PicoPure RNA Isolation Kit (ThermoFisher Scientific, Cat. #: KIT0202, KIT0204) was used for RNA extraction based on the manufacturer's instructions. After RNA extraction, iScript cDNA Synthesis Kit (BioRad) was employed for the cDNA synthesis. Two mice (4 inguino-axillary lymphatic vessels) were used per RNA extraction reaction. The cDNA from multiple extraction reactions was pooled in a single cDNA master tube. Next, real-time PCR for *Myh11* and *Acta2* was performed according to the manufacturer's instructions using iTaq Universal SYBR Green Supermix (Bio-Rad, Cat. #: 1725124) on a Bio-Rad CFX Connect Real-Time PCR Detection System.

Gene	**Forward Primer**	**Reverse Primer**
Gapdh	AGGTCGGTGTGAACGGATTTG	TGTAGACCATGTAGTTGAGGTCA
β-Actin	GGCTGTATTCCCCTCCATCG	CCAGTTGGTAACAATGCCATGT
Acta2	CCTCATGAAGATCCTGACTG	GTTCGTTTCCAATGGTGATC
Myh11	CAAGAAACTGGAGGATGACA	TCATAGACTCATGCTTGCTC

Staining of whole mount collecting lymphatic vessels

For αSMA whole mount staining, inguino-axillary lymphatic vessels or the afferent collecting lymphatic vessels to the popliteal lymph node were collected as described above. Next, the isolated vessels were fixed for two hours at room temperature in 4% formaldehyde, washed three times in 1x PBS for 15 minutes, then stored in 1x PBS at 4°C for overnight. The following day, the lymphatic vessels were blocked and permeabilized for 3 hours at room temperature in 10% normal donkey serum (NDS) and 0.1% Triton-X in PBS. After that, lymphatic vessels were washed in 1x PBS three times, with each wash lasting 5 minutes. Next, lymphatic vessels were carefully cut into smaller pieces and stained with αSMA-Cy3 (1/200 dilution, Clone: 1A4, MilliporeSigma, Cat. #: C6198) and DAPI in 1x PBS with 1% NDS and 0.05% Triton-X at 4°C for overnight. The following day, lymphatic vessels were washed in 1x PBS at room temperature three times, with each wash lasting 15 minutes. After that, the lymphatic vessels were mounted onto glass slides using ProlongGold liquid mountant and glass coverslips. Slides were cured flat on the benchtop at room temperature for at least 48 hours prior to imaging. Samples were imaged using a Zeiss LSM 880 Airyscan confocal microscope with 40x oil objective at one Airyunit.

For Notch3 and αSMA wholemount staining, the afferent collecting lymphatic vessels to the popliteal lymph node were collected from Prox1-GFP mice as described above. The popliteal lymphatic vessels were fixed with 4% PFA for 30 minutes, washed with 1x PBS, and incubated with antibodies and DAPI overnight at 4°C (Notch3-APC, 1/50 dilution, Clone: HMN3-133, Biolegend, Cat:130512; aSMA-Cy3, 1/200 dilution, Clone: 1A4, MilliporeSigma Cat: C6198). The following day, lymphatic vessels were washed three times in 1x PBS, with each wash lasting 5 minutes. The tissue was then placed on a glass slide to visualize lymphatic vessels using a confocal microscope (Olympus 1X81) with 4x, 10x, and 20x air objectives, and 60x oil objectives (Olympus). The raw image data in multi-tiff format were processed by ImageJ.

Intravital lymphatic pumping assay

Mice were anesthetized using ketamine (100 mg/kg) and xylazine (10 mg/kg). 3 μL of 2% FITC-Dextran (2 million molecular weight) in 0.9% normal saline was injected intradermally into the

footpad. The surgical site was prepared by carefully removing the skin and underlying connective tissue near the afferent lymphatic vessel leading to the popliteal lymph node (PLV) as described previously (Jones et al., 2018; Liao et al., 2011, 2014). Time-lapse imaging was performed using an inverted fluorescence microscope (Olympus Ix70) to record 2250 images at 133 ms intervals. Custom MATLAB code was employed for image analysis. The vessel wall position was tracked, and frequency and ejection fraction was measured using a peak-and-valley method as described previously (Liao et al., 2014). Ejection fraction serves as a measure of the strength of lymphatic contraction.

In vitro assay of lymphatic muscle cell response to TNFα

The collecting lymphatic vessels in young mice (6-week-old) were isolated according to previously described methods with slight modifications (Arroyo-Ataz and Jones, 2022). Briefly, mice were anesthetized with ketamine (100 mg/kg) and xylazine (10 mg/kg) followed by a footpad injection of 4 μL 4% Evans Blue Dye to visualize the lymphatic vessels. After that, the surgical site was shaved and prepared by removing the skin and underlying connective tissue to expose the afferent lymphatic vessel to the popliteal lymph node. The isolated lymphatic vessels were digested for 30 minutes at 37ºC with agitation in an enzymatic cocktail consisting of 1 mg/mL collagenase I (Worthington, Cat. #: LS004196), 1 mg/mL Dispase II (Gibco, Cat. #: 17105041), 100 μg/ml DNAse I (Millipore Sigma, Cat. #: 04716728001) and 200 μg/ml Liberase (Millipore Sigma, Cat. #: 05401020001). The digestion was quenched with 10% FBS and resuspended in 20% FBS DMEM (0.5 ml per animal). Cells were plated in a 24-well plate and grown for 4-5 days, after which they were treated with TNFα (Biolegend, Cat. #: 575202) for 24-48 hours. Cells were pelleted and then resuspended in RLT lysis buffer. RNA was extracted using a Qiagen RNeasy kit (Qiagen, Cat. #: 74004) based on the manufacturer's instructions. Verso cDNA Synthesis Kit (Thermo Scientific, AB1453A) was employed for cDNA synthesis. Next, real-time PCR for *Myh11* and *Acta2* was performed according to the manufacturer's instructions using iTaq Universal SYBR Green Supermix (Bio-Rad, Cat. #: 1725124) on a Bio-Rad CFX Connect Real-Time PCR Detection System.

Statistical analysis

Unpaired t-tests and one-way ANOVA were performed within each group to determine statistical significance, with an alpha value of 0.05. All statistical analyses were carried out using Prism Version 9 Software (GraphPad).

Data availability

The authors confirm that all other data supporting the findings of this study are available within the paper and its supplementary information files.

Acknowledgments

We thank Ulandt Kim from the NextGen core at Massachusetts General Hospital for the help with single-cell sequencing. We thank Carolyn Smith for outstanding technical support of the immunohistochemistry studies. We thank Dr. Mario Suvá of Massachusetts General Hospital and Dr. Carrie Shawber of Columbia University for important discussions.

Funding

T.P.P. is supported by grants from the NIH (R21AI097745, R01CA214913, R01HL128168, R01CA284372, and R01CA284603), and the Rullo Family MGH Research Scholar Award. K.J.R.

is supported by grants from the NIH (T32 GM007592), the International Anesthesia Research Society, and the Harvard University Eleanor and Miles Shore Faculty Development Award. M.J.O. is supported by a grant from the NIH F32CA275298. H.Z. is supported by a grant from the NIH K00CA234940. L.M. is supported by a grant from the Walter Benjamin Programme, Deutsche Forschunsgemeinschaft Nr.: ME5486/1-2. M.S.R is supported by a grant from the NIH F32HL156654. A.S.K. is supported by a grant from the Agency for Science, Technology and Research (A*STAR) graduate scholarship. E.M.B. was supported by a fellowship from the Lipedema Foundation. D.J. is supported by a career development grant from the American Association for Cancer Research and Breast Cancer Research Foundation. J. M. U. is supported by the Melanoma Research Foundation and Breast Cancer Research Alliance. J.W.B. is supported by NIH grant R01CA284603. L.L.M. is supported by a grant from the NIH (R01CA284603).

Author contributions

Research design: T.P.P., P.L., K.J.R., K.R., E.R.P. Research performance: P.L., K.J.R., J.J.R, K.R., M.J.O, E.M.B., M.M., A.S.K., G.A.A., M.S.R., H.Z., L.M., M.D., D.J. Data analysis: P.L., K.J.R., M.J.O, E.M.B., A.S.K., G.A.A. Supervision: T.P.P. Writing – original draft: P.L. Writing – review & editing: P.L., K.J.R., J.J.R, M.J.O, A.S.K., L.M., H.K., J.W.B, J.M.U., L.L.M., D.J., T.P.P.

Conflict of interest

The authors declare that they have no competing interests. Lance L. Munn receives equity from Bayer and consultants for SimBiosys. Hengbo Zhou serves as a "Scientific consultant" for AOA dx. Echoe M. Bouta is currently an employee at Takeda.

Reference

Akl, T.J., Nagai, T., Coté, G.L., and Gashev, A.A. (2011). Mesenteric lymph flow in adult and aged rats. Am. J. Physiol. - Hear. Circ. Physiol. *301*, 1828–1840.

Alitalo, K. (2011). The lymphatic vasculature in disease. Nat. Med. *17*, 1371–1380.

Arroyo-Ataz, G., and Jones, D. (2022). Dissection of murine collecting lymphatic vessels for imaging, single-cell analysis, and tissue culture of lymphatic muscle cells. STAR Protoc. *3*, 101800.

Aspelund, A., Robciuc, M.R., Karaman, S., Makinen, T., and Alitalo, K. (2016). Lymphatic System in Cardiovascular Medicine. Circ. Res. *118*, 515–530.

Baluk, P., Fuxe, J., Hashizume, H., Romano, T., Lashnits, E., Butz, S., Vestweber, D., Corada, M., Molendini, C., Dejana, E., et al. (2007). Functionally specialized junctions between endothelial cells of lymphatic vessels. J. Exp. Med. *204*, 2349–2362.

Banerji, S., Ni, J., Wang, S.X., Clasper, S., Su, J., Tammi, R., Jones, M., and Jackson, D.G. (1999). LYVE-1, a new homologue of the CD44 glycoprotein, is a lymph-specific receptor for hyaluronan. J. Cell Biol. *144*, 789–801.

Bartleson, J.M., Radenkovic, D., Covarrubias, A.J., Furman, D., Winer, D.A., and Verdin, E. (2021). SARS-CoV-2, COVID-19 and the aging immune system. Nat. Aging *1*, 769–782.

Beckett, E.A.H., Hollywood, M.A., Thornbury, K.D., and McHale, N.G. (2007). Spontaneous electrical activity in sheep mesenteric lymphatics. Lymphat. Res. Biol. *5*, 29–43.

Biswas, L., Chen, J., De Angelis, J., Singh, A., Owen-Woods, C., Ding, Z., Pujol, J.M., Kumar, N., Zeng, F., Ramasamy, S.K., et al. (2023). Lymphatic vessels in bone support regeneration after injury. Cell *186*, 382-397.e24.

Blanco-Carmona, E. (2022). Generating publication ready visualizations for Single Cell transcriptomics using SCpubr. BioRxiv 2022.02.28.482303.

Bochaton-Piallat, M.L., Clowes, A.W., Clowes, M.M., Fischer, J.W., Redard, M., Gabbiani, F., and Gabbiani, G. (2001). Cultured arterial smooth muscle cells maintain distinct phenotypes when implanted into carotid artery. Arterioscler. Thromb. Vasc. Biol. *21*, 949–954.

Breslin, J.W., Yang, Y., Scallan, J.P., Sweat, R.S., Adderley, S.P., and Murfee, W.L. (2019). Lymphatic vessel network structure and physiology. Compr. Physiol. *9*, 207–299.

Bridenbaugh, E.A., Nizamutdinova, I.T., Jupiter, D., Nagai, T., Thangaswamy, S., Chatterjee, V., and Gashev, A.A. (2013). Lymphatic muscle cells in rat mesenteric lymphatic vessels of various ages. Lymphat. Res. Biol. *11*, 35–42.

Brouillard, P., Witte, M.H., Erickson, R.P., Damstra, R.J., Becker, C., Quéré, I., and Vikkula, M. (2021). Primary lymphoedema. Nat. Rev. Dis. Prim. *7*, 77.

Butler, M.G., Isogai, S., and Weinstein, B.M. (2009). Lymphatic development. Birth Defects Res. C. Embryo Today *87*, 222–231.

Cao, E., Watt, M.J., Nowell, C.J., Quach, T., Simpson, J.S., De Melo Ferreira, V., Agarwal, S., Chu, H., Srivastava, A., Anderson, D., et al. (2021). Mesenteric lymphatic dysfunction promotes insulin resistance and represents a potential treatment target in obesity. Nat. Metab. *3*, 1175–1188.

Castorena-Gonzalez, J.A., Zawieja, S.D., Li, M., Srinivasan, R.S., Simon, A.M., de Wit, C., de la Torre, R., Martinez-Lemus, L.A., Hennig, G.W., and Davis, M.J. (2018). Mechanisms of Connexin-Related Lymphedema. Circ. Res. *123*, 964–985.

Chachaj, A., Puła, B., Chabowski, M., Grzegrzółka, J., Szahidewicz-Krupska, E., Karczewski, M., Janczak, D., Dzięgiel, P., Podhorska-Okołów, M., Mazur, G., et al. (2018). Role of the Lymphatic System in the Pathogenesis of Hypertension in Humans. Lymphat. Res. Biol. *16*, 140–146.

Chan, A.K., and von der Weid, P.-Y. (2003). 5-HT decreases contractile and electrical activities in lymphatic vessels of the guinea-pig mesentery: role of 5-HT 7-receptors. Br. J. Pharmacol. *139*, 243–254.

Chen, Y., Rehal, S., Roizes, S., Zhu, H.L., Cole, W.C., and von der Weid, P.Y. (2017). The pro-inflammatory cytokine TNF-α inhibits lymphatic pumping via activation of the NF-κB-iNOS signaling pathway. Microcirculation *24*, 1–13.

Cohen, M., Giladi, A., Gorki, A.D., Solodkin, D.G., Zada, M., Hladik, A., Miklosi, A., Salame, T.M., Halpern, K.B., David, E., et al. (2018). Lung Single-Cell Signaling Interaction Map Reveals Basophil Role in Macrophage Imprinting. Cell *175*, 1031-1044.e18.

David, J.-P., Stas, J.I., Schmitt, N., and Bocksteins, E. (2015). Auxiliary KCNE subunits modulate both homotetrameric Kv2.1 and heterotetrameric Kv2.1/Kv6.4 channels. Sci. Rep. *5*, 12813.

Davis, M.J., Kim, H.J., and Nichols, C.G. (2022). KATP channels in lymphatic function. Am. J. Physiol. - Cell Physiol. *323*, C1018–C1035.

Davis, M.J., Castorena-Gonzalez, J.A., Kim, H.J., Li, M., Remedi, M., and Nichols, C.G. (2023a). Lymphatic contractile dysfunction in mouse models of Cantú Syndrome with K(ATP) channel gain-of-function. Funct. (Oxford, England) *4*, zqad017.

Davis, M.J., Kim, H.J., Li, M., and Zawieja, S.D. (2023b). A vascular smooth muscle-specific integrin-α8 Cre mouse for lymphatic contraction studies that allows male-female comparisons and avoids visceral myopathy. Front. Physiol. *13*, 1–10.

Ducoli, L., and Detmar, M. (2021). Beyond PROX1: transcriptional, epigenetic, and noncoding RNA regulation of lymphatic identity and function. Dev. Cell *56*, 406–426.

Felder, E., Protasi, F., Hirsch, R., Franzini-Armstrong, C., and Allen, P.D. (2002). Morphology and molecular composition of sarcoplasmic reticulum surface junctions in the absence of DHPR and RyR in mouse skeletal muscle. Biophys. J. *82*, 3144–3149.

Fujimoto, N., He, Y., D'Addio, M., Tacconi, C., Detmar, M., and Dieterich, L.C. (2020). Single-cell mapping reveals new markers and functions of lymphatic endothelial cells in lymph nodes. PLoS Biol. *18*.

Gashev, A.A. (2010). Basic mechanisms controlling lymph transport in the mesenteric lymphatic net. Ann. N. Y. Acad. Sci. *1207 Suppl*, E16-20.

Ge, S.X., Jung, D., and Yao, R. (2020). ShinyGO: a graphical gene-set enrichment tool for animals and plants. Bioinformatics *36*, 2628–2629.

González-Loyola, A., and Petrova, T. V. (2021). Development and aging of the lymphatic vascular system. Adv. Drug Deliv. Rev. *169*, 63–78.

Goodyer, W.R., Beyersdorf, B.M., Duan, L., van den Berg, N.S., Mantri, S., Galdos, F.X., Puluca,

N., Buikema, J.W., Lee, S., Salmi, D., et al. (2022). In vivo visualization and molecular targeting of the cardiac conduction system. J. Clin. Invest. *132*.

Grant, A.O. (2009). Cardiac ion channels. Circ. Arrhythm. Electrophysiol. *2*, 185–194.

Grimm, L., Mason, E., Yu, H., Dudczig, S., Panara, V., Chen, T., Bower, N.I., Paterson, S., Rondon Galeano, M., Kobayashi, S., et al. (2023). Single-cell analysis of lymphatic endothelial cell fate specification and differentiation during zebrafish development. EMBO J. *42*, e112590.

Gutierrez-Miranda, L., and Yaniv, K. (2020). Cellular Origins of the Lymphatic Endothelium: Implications for Cancer Lymphangiogenesis. Front. Physiol. *11*, 1–16.

Hadizadeh, M., Mohaddes Ardebili, S.M., Salehi, M., Young, C., Mokarian, F., McClellan, J., Xu, Q., Kazemi, M., Moazam, E., Mahaki, B., et al. (2018). GJA4/Connexin 37 Mutations Correlate with Secondary Lymphedema Following Surgery in Breast Cancer Patients. Biomedicines *6*.

Hald, B.O., Castorena-Gonzalez, J.A., Zawieja, S.D., Gui, P., and Davis, M.J. (2018). Electrical Communication in Lymphangions. Biophys. J. *115*, 936–949.

Han, X., Wang, R., Zhou, Y., Fei, L., Sun, H., Lai, S., Saadatpour, A., Zhou, Z., Chen, H., Ye, F., et al. (2018). Mapping the Mouse Cell Atlas by Microwell-Seq. Cell *172*, 1091-1107.e17.

Hollywood, M.A., Cotton, K.D., Thornbury, K.D., and McHale, N.G. (1997). Tetrodotoxin-sensitive sodium current in sheep lymphatic smooth muscle. J. Physiol. *503 (Pt 1*, 13–20.

Hong, Y.-K., Harvey, N., Noh, Y.-H., Schacht, V., Hirakawa, S., Detmar, M., and Oliver, G. (2002). Prox1 is a master control gene in the program specifying lymphatic endothelial cell fate. Dev. Dyn. an Off. Publ. Am. Assoc. Anat. *225*, 351–357.

Itkin, M., Rockson, S.G., and Burkhoff, D. (2021). Pathophysiology of the Lymphatic System in Patients With Heart Failure: JACC State-of-the-Art Review. J. Am. Coll. Cardiol. *78*, 278–290.

Jackson, D.G., Prevo, R., Clasper, S., and Banerji, S. (2001). LYVE-1, the lymphatic system and tumor lymphangiogenesis. Trends Immunol. *22*, 317–321.

Jiang, X., Tian, W., Nicolls, M.R., and Rockson, S.G. (2019). The Lymphatic System in Obesity, Insulin Resistance, and Cardiovascular Diseases. Front. Physiol. *10*, 1402.

Jin, S., Guerrero-Juarez, C.F., Zhang, L., Chang, I., Ramos, R., Kuan, C.H., Myung, P., Plikus, M. V., and Nie, Q. (2021). Inference and analysis of cell-cell communication using CellChat. Nat. Commun. *12*, 1–20.

Jo, M., Trujillo, A.N., Yang, Y., and Breslin, J.W. (2019). Evidence of functional ryanodine receptors in rat mesenteric collecting lymphatic vessels. Am. J. Physiol. Heart Circ. Physiol. *317*, H561–H574.

Jones, D., Meijer, E.F.J., Blatter, C., Liao, S., Pereira, E.R., Bouta, E.M., Jung, K., Chin, S.M., Huang, P., Munn, L.L., et al. (2018). Methicillin resistant Staphylococcus aureus causes sustained collecting lymphatic vessel dysfunction. Sic Transl Med *1*.

Kaipainen, A., Korhonen, J., Mustonen, T., van Hinsbergh, V.W., Fang, G.H., Dumont, D., Breitman, M., and Alitalo, K. (1995). Expression of the fms-like tyrosine kinase 4 gene becomes restricted to lymphatic endothelium during development. Proc. Natl. Acad. Sci. U. S. A. *92*, 3566–3570.

Kalucka, J., de Rooij, L.P.M.H., Goveia, J., Rohlenova, K., Dumas, S.J., Meta, E., Conchinha, N. V., Taverna, F., Teuwen, L.A., Veys, K., et al. (2020). Single-Cell Transcriptome Atlas of Murine Endothelial Cells. Cell *180*, 764-779.e20.

Kanady, J.D., Dellinger, M.T., Munger, S.J., Witte, M.H., and Simon, A.M. (2011). Connexin37 and Connexin43 deficiencies in mice disrupt lymphatic valve development and result in lymphatic disorders including lymphedema and chylothorax. Dev. Biol. *354*, 253–266.

Kanaya, N., Chang, G., Wu, X., Saeki, K., Bernal, L., Shim, H.J., Wang, J., Warden, C., Yamamoto, T., Li, J., et al. (2019). Single-cell RNA-sequencing analysis of estrogen- and endocrine-disrupting chemical-induced reorganization of mouse mammary gland. Commun. Biol. *2*, 1–15.

Karaayvaz, M., Cristea, S., Gillespie, S.M., Patel, A.P., Mylvaganam, R., Luo, C.C., Specht, M.C., Bernstein, B.E., Michor, F., and Ellisen, L.W. (2018). Unravelling subclonal heterogeneity and aggressive disease states in TNBC through single-cell RNA-seq. Nat. Commun. *9*.

Kataru, R.P., Park, H.J., Shin, J., Baik, J.E., Sarker, A., Brown, S., and Mehrara, B.J. (2022). Structural and Functional Changes in Aged Skin Lymphatic Vessels. Front. Aging *3*, 1–13.

Kenney, H.M., Bell, R.D., Masters, E.A., Xing, L., Ritchlin, C.T., and Schwarz, E.M. (2020). Lineage tracing reveals evidence of a popliteal lymphatic muscle progenitor cell that is distinct from skeletal and vascular muscle progenitors. Sci. Rep. *10*, 1–11.

Kenney, H.M., Wu, C.L., Loiselle, A.E., Xing, L., Ritchlin, C.T., and Schwarz, E.M. (2022). Single-cell transcriptomics of popliteal lymphatic vessels and peripheral veins reveals altered lymphatic muscle and immune cell populations in the TNF-Tg arthritis model. Arthritis Res. Ther. *24*, 1–20.

Kenney, H.M., Peng, Y., de Mesy Bentley, K.L., Xing, L., Ritchlin, C.T., and Schwarz, E.M. (2023). The Enigmas of Lymphatic Muscle Cells: Where Do They Come From, How Are They Maintained, and Can They Regenerate? Curr. Rheumatol. Rev. *19*, 246–259.

Kim, H.J., Li, M., Erlich, E.C., Randolph, G.J., and Davis, M.J. (2023). ERG K(+) channels mediate a major component of action potential repolarization in lymphatic muscle. Sci. Rep. *13*, 14890.

Kim, H.R., Appel, S., Vetterkind, S., Gangopadhyay, S.S., and Morgan, K.G. (2008). Smooth muscle signalling pathways in health and disease. J. Cell. Mol. Med. *12*, 2165–2180.

Klaourakis, K., Vieira, J.M., and Riley, P.R. (2021). The evolving cardiac lymphatic vasculature in development, repair and regeneration. Nat. Rev. Cardiol. *18*, 368–379.

Kukk, E., Lymboussaki, A., Taira, S., Kaipainen, A., Jeltsch, M., Joukov, V., and Alitalo, K. (1996). VEGF-C receptor binding and pattern of expression with VEGFR-3 suggests a role in lymphatic vascular development. Development *122*, 3829–3837.

Lee, A.S., de Lencastre, H., Garau, J., Kluytmans, J., Malhotra-Kumar, S., Peschel, A., and Harbarth, S. (2018). Methicillin-resistant Staphylococcus aureus. Nat. Rev. Dis. Prim. *4*, 18033.

Lee, S., Roizes, S., and von der Weid, P.-Y. (2014). Distinct roles of L- and T-type voltage-dependent Ca2+ channels in regulation of lymphatic vessel contractile activity. J. Physiol. *592*, 5409–5427.

Lee, Y., Zawieja, S.D., and Muthuchamy, M. (2022). Lymphatic Collecting Vessel: New Perspectives on Mechanisms of Contractile Regulation and Potential Lymphatic Contractile Pathways to Target in Obesity and Metabolic Diseases. Front. Pharmacol. *13*, 848088.

Leuranguer, V., Mangoni, M.E., Nargeot, J., and Richard, S. (2001). Inhibition of T-type and L-type calcium channels by mibefradil: physiologic and pharmacologic bases of cardiovascular effects. J. Cardiovasc. Pharmacol. *37*, 649–661.

Li, C.M.C., Shapiro, H., Tsiobikas, C., Selfors, L.M., Chen, H., Rosenbluth, J., Moore, K., Gupta, K.P., Gray, G.K., Oren, Y., et al. (2020). Aging-Associated Alterations in Mammary Epithelia and Stroma Revealed by Single-Cell RNA Sequencing. Cell Rep. *33*, 108566.

Liao, S., Cheng, G., Conner, D.A., Huang, Y., Kucherlapati, R.S., Munn, L.L., Ruddle, N.H., Jain, R.K., Fukumura, D., and Padera, T.P. (2011). Impaired lymphatic contraction associated with immunosuppression. Proc. Natl. Acad. Sci. U. S. A. *108*, 18784–18789.

Liao, S., Jones, D., Cheng, G., and Padera, T.P. (2014). Method for the quantitative measurement of collecting lymphatic vessel contraction in mice. J. Biol. Methods *1*.

Liberzon, A., Birger, C., Thorvaldsdóttir, H., Ghandi, M., Mesirov, J.P., and Tamayo, P. (2015). The Molecular Signatures Database Hallmark Gene Set Collection. Cell Syst. *1*, 417–425.

Liu, X., Chen, W., Li, W., Li, Y., Priest, J.R., Zhou, B., Wang, J., and Zhou, Z. (2019). Single-Cell RNA-Seq of the Developing Cardiac Outflow Tract Reveals Convergent Development of the Vascular Smooth Muscle Cells. Cell Rep. *28*, 1346-1361.e4.

Liu, X., De la Cruz, E., Gu, X., Balint, L., Oxendine-Burns, M., Terrones, T., Ma, W., Kuo, H.-H., Lantz, C., Bansal, T., et al. (2020). Lymphoangiocrine signals promote cardiac growth and repair. Nature *588*, 705–711.

Louveau, A., Smirnov, I., Keyes, T.J., Eccles, J.D., Rouhani, S.J., Peske, J.D., Derecki, N.C., Castle, D., Mandell, J.W., Lee, K.S., et al. (2015). Structural and functional features of central nervous system lymphatic vessels. Nature *523*, 337–341.

Louveau, A., Herz, J., Alme, M.N., Salvador, A.F., Dong, M.Q., Viar, K.E., Herod, S.G., Knopp, J., Setliff, J.C., Lupi, A.L., et al. (2018). CNS lymphatic drainage and neuroinflammation are regulated by meningeal lymphatic vasculature. Nat. Neurosci. *21*, 1380–1391.

Luecken, M.D., and Theis, F.J. (2019). Current best practices in single-cell RNA-seq analysis: a tutorial. Mol. Syst. Biol. *15*.

Majgaard, J., Skov, F.G., Kim, S., Hjortdal, V.E., and Boedtkjer, D.M.B. (2022). Positive chronotropic action of HCN channel antagonism in human collecting lymphatic vessels. Physiol. Rep. *10*, e15401.

Mäkinen, T., Boon, L.M., Vikkula, M., and Alitalo, K. (2021). Lymphatic Malformations: Genetics, Mechanisms and Therapeutic Strategies. Circ. Res. *129*, 136–154.

Marbán, E. (2002). Cardiac channelopathies. Nature *415*, 213–218.

Martin-Almedina, S., Mortimer, P.S., and Ostergaard, P. (2021). Development and physiological functions of the lymphatic system: insights from human genetic studies of primary lymphedema. Physiol. Rev. *101*, 1809–1871.

McCloskey, K.D., Toland, H.M., Hollywood, M.A., Thornbury, K.D., and McHale, N.G. (1999).

Hyperpolarisation-activated inward current in isolated sheep mesenteric lymphatic smooth muscle. J. Physiol. *521 Pt 1*, 201–211.

Meens, M.J., Sabine, A., Petrova, T. V, and Kwak, B.R. (2014). Connexins in lymphatic vessel physiology and disease. FEBS Lett. *588*, 1271–1277.

Da Mesquita, S., Louveau, A., Vaccari, A., Smirnov, I., Cornelison, R.C., Kingsmore, K.M., Contarino, C., Onengut-Gumuscu, S., Farber, E., Raper, D., et al. (2018). Functional aspects of meningeal lymphatics in ageing and Alzheimer's disease. Nature *560*, 185–191.

De Micheli, A.J., Laurilliard, E.J., Heinke, C.L., Ravichandran, H., Fraczek, P., Soueid-Baumgarten, S., De Vlaminck, I., Elemento, O., and Cosgrove, B.D. (2020). Single-Cell Analysis of the Muscle Stem Cell Hierarchy Identifies Heterotypic Communication Signals Involved in Skeletal Muscle Regeneration. Cell Rep. *30*, 3583-3595.e5.

Moreira, S.B., Baptista, J.P., Gonçalves-Pereira, J., Pereira, J.M., Ribeiro, O., Dias, C.C., Froes, F., and Paiva, J.-A. (2021). Impact of age in critically Ill infected patients: a post-hoc analysis of the INFAUCI study. Eur. Geriatr. Med. *12*, 1057–1064.

Morfoisse, F., Tatin, F., Chaput, B., Therville, N., Vaysse, C., Métivier, R., Malloizel-Delaunay, J., Pujol, F., Godet, A.-C., De Toni, F., et al. (2018). Lymphatic Vasculature Requires Estrogen Receptor-α Signaling to Protect From Lymphedema. Arterioscler. Thromb. Vasc. Biol. *38*, 1346–1357.

Morfoisse, F., Zamora, A., Marchaud, E., Nougue, M., Diallo, L.H., David, F., Roussel, E., Lacazette, E., Prats, A.C., Tatin, F., et al. (2021). Sex hormones in lymphedema. Cancers (Basel). *13*, 1–16.

Muhl, L., Genové, G., Leptidis, S., Liu, J., He, L., Mocci, G., Sun, Y., Gustafsson, S., Buyandelger, B., Chivukula, I. V., et al. (2020). Single-cell analysis uncovers fibroblast heterogeneity and criteria for fibroblast and mural cell identification and discrimination. Nat. Commun. *11*, 1–18.

Muhl, L., Mocci, G., Pietilä, R., Liu, J., He, L., Genové, G., Leptidis, S., Gustafsson, S., Buyandelger, B., Raschperger, E., et al. (2022). A single-cell transcriptomic inventory of murine smooth muscle cells. Dev. Cell *57*, 2426-2443.e6.

Muthuchamy, M., Gashev, A., Boswell, N., Dawson, N., and Zawieja, D. (2003). Molecular and functional analyses of the contractile apparatus in lymphatic muscle. FASEB J. *17*, 920–922.

Nagai, T., Bridenbaugh, E.A., and Gashev, A.A. (2011). Aging-associated alterations in contractility of rat mesenteric lymphatic vessels. Microcirculation *18*, 463–473.

Negrini, D., Marcozzi, C., Solari, E., Bossi, E., Cinquetti, R., Reguzzoni, M., and Moriondo, A. (2016). Hyperpolarization-activated cyclic nucleotide-gated channels in peripheral diaphragmatic lymphatics. Am. J. Physiol. Heart Circ. Physiol. *311*, H892–H903.

Nomura, S., Satoh, M., Fujita, T., Higo, T., Sumida, T., Ko, T., Yamaguchi, T., Tobita, T., Naito, A.T., Ito, M., et al. (2018). Cardiomyocyte gene programs encoding morphological and functional signatures in cardiac hypertrophy and failure. Nat. Commun. *9*, 4435.

Norden, P.R., and Kume, T. (2020). The Role of Lymphatic Vascular Function in Metabolic Disorders. Front. Physiol. *11*, 1–16.

Ohhashi, T., McHale, N.G., Roddie, I.C., and Thornbury, K.D. (1980). Electrical field stimulation

as a method of stimulating nerve or smooth muscle in isolated bovine mesenteric lymphatics. Pflugers Arch. *388*, 221–226.

Oliver, G., Kipnis, J., Randolph, G.J., and Harvey, N.L. (2020). The Lymphatic Vasculature in the 21st Century: Novel Functional Roles in Homeostasis and Disease. Cell *182*, 270–296.

Padera, T.P., Meijer, E.F.J., and Munn, L.L. (2016). The Lymphatic System in Disease Processes and Cancer Progression. Annu. Rev. Biomed. Eng. *18*, 125–158.

Pereira da Silva, E.A., Martín-Aragón Baudel, M., Navedo, M.F., and Nieves-Cintrón, M. (2022). Ion channel molecular complexes in vascular smooth muscle. Front. Physiol. *13*, 1–11.

Petrova, T. V., and Koh, G.Y. (2018). Organ-specific lymphatic vasculature: From development to pathophysiology. J. Exp. Med. *215*, 35–49.

Petrova, T. V., and Koh, G.Y. (2020). Biological functions of lymphatic vessels. Science (80-.). *369*.

Petrova, T. V, Mäkinen, T., Mäkelä, T.P., Saarela, J., Virtanen, I., Ferrell, R.E., Finegold, D.N., Kerjaschki, D., Ylä-Herttuala, S., and Alitalo, K. (2002). Lymphatic endothelial reprogramming of vascular endothelial cells by the Prox-1 homeobox transcription factor. EMBO J. *21*, 4593–4599.

Razavi, M.S., Lei, J., Bucknell, J.B., Padera, T., and Munn, L. (2023). Regeneration of collecting lymphatic vessels following injury.

Reed, H.O., Wang, L., Sonett, J., Chen, M., Yang, J., Li, L., Aradi, P., Jakus, Z., D'Armiento, J., Hancock, W.W., et al. (2019). Lymphatic impairment leads to pulmonary tertiary lymphoid organ formation and alveolar damage. J. Clin. Invest. *129*, 2514–2526.

Rehal, S., Stephens, M., Roizes, S., Liao, S., and von der Weid, P.-Y. (2018). Acute small intestinal inflammation results in persistent lymphatic alterations. Am. J. Physiol. Gastrointest. Liver Physiol. *314*, G408–G417.

Rehal, S., Kataru, R.P., Hespe, G.E., Baik, J.E., Park, H.J., Ly, C., Shin, J.Y., and Mehrara, B.J. (2020). Regulation of lymphatic function and injury by nitrosative stress in obese mice. Mol. Metab. *42*, 101081.

Renner, S.W., Walker, L.M., Forsberg, L.J., Sexton, J.Z., and Brenman, J.E. (2017). Carbonic anhydrase III (Car3) is not required for fatty acid synthesis and does not protect against high-fat diet induced obesity in mice. PLoS One *12*, e0176502.

Rensen, S.S.M., Doevendans, P.A.F.M., and Van Eys, G.J.J.M. (2007). Regulation and characteristics of vascular smooth muscle cell phenotypic diversity. Netherlands Hear. J. *15*, 100–108.

Rockson, S.G. (2018). Lymphedema after Breast Cancer Treatment. N. Engl. J. Med. *379*, 1937–1944.

Rockson, S.G. (2021). Advances in Lymphedema. Circ. Res. *128*, 2003–2016.

Rodda, L.B., Lu, E., Bennett, M.L., Sokol, C.L., Wang, X., Luther, S.A., Barres, B.A., Luster, A.D., Ye, C.J., and Cyster, J.G. (2018). Single-Cell RNA Sequencing of Lymph Node Stromal Cells Reveals Niche-Associated Heterogeneity. Immunity *48*, 1014-1028.e6.

Russell, P.S., Hong, J., Trevaskis, N.L., Windsor, J.A., Martin, N.D., and Phillips, A.R.J. (2022). Lymphatic contractile function: A comprehensive review of drug effects and potential clinical application. Cardiovasc. Res. *118*, 2437–2457.

Scallan, J.P., Zawieja, S.D., Castorena-Gonzalez, J.A., and Davis, M.J. (2016). Lymphatic pumping: mechanics, mechanisms and malfunction. J. Physiol. *594*, 5749–5768.

Siret, C., van Lessen, M., Bavais, J., Jeong, H.W., Reddy Samawar, S.K., Kapupara, K., Wang, S., Simic, M., de Fabritus, L., Tchoghandjian, A., et al. (2022). Deciphering the heterogeneity of the Lyve1+ perivascular macrophages in the mouse brain. Nat. Commun. *13*, 7366.

Smeltzer, D.M., Stickler, G.B., and Schirger, A. (1985). Primary lymphedema in children and adolescents: a follow-up study and review. Pediatrics *76*, 206–218.

Smoot, B., Kober, K.M., Paul, S.M., Levine, J.D., Abrams, G., Mastick, J., Topp, K., Conley, Y.P., and Miaskowski, C.A. (2017). Potassium Channel Candidate Genes Predict the Development of Secondary Lymphedema Following Breast Cancer Surgery. Nurs. Res. *66*, 85–94.

Solari, E., Marcozzi, C., Negrini, D., and Moriondo, A. (2023). Fluid Osmolarity Modulates the Rate of Spontaneous Contraction of Lymphatic Vessels and Lymph Flow by Means of a Cooperation between TRPV and VRAC Channels. Biology (Basel). *12*.

Stolarz, A.J., Sarimollaoglu, M., Marecki, J.C., Fletcher, T.W., Galanzha, E.I., Rhee, S.W., Zharov, V.P., Klimberg, V.S., and Rusch, N.J. (2019). Doxorubicin Activates Ryanodine Receptors in Rat Lymphatic Muscle Cells to Attenuate Rhythmic Contractions and Lymph Flow. J. Pharmacol. Exp. Ther. *371*, 278–289.

Stuart, T., Butler, A., Hoffman, P., Hafemeister, C., Papalexi, E., Mauck III, W.M., Hao, Y., Stoeckius, M., Smibert, P., and Satija, R. (2019). Comprehensive Integration of Single-Cell Data. Cell *177*, 1888-1902.e21.

Sweeney, H.L., and Hammers, D.W. (2018). Muscle Contraction. Cold Spring Harb. Perspect. Biol. *10*, a023200.

Takeda, A., Hollmén, M., Dermadi, D., Pan, J., Brulois, K.F., Kaukonen, R., Lönnberg, T., Boström, P., Koskivuo, I., Irjala, H., et al. (2019). Single-Cell Survey of Human Lymphatics Unveils Marked Endothelial Cell Heterogeneity and Mechanisms of Homing for Neutrophils. Immunity *51*, 561-572.e5.

Telinius, N., Mohanakumar, S., Majgaard, J., Kim, S., Pilegaard, H., Pahle, E., Nielsen, J., de Leval, M., Aalkjaer, C., Hjortdal, V., et al. (2014a). Human lymphatic vessel contractile activity is inhibited in vitro but not in vivo by the calcium channel blocker nifedipine. J. Physiol. *592*, 4697–4714.

Telinius, N., Kim, S., Pilegaard, H., Pahle, E., Nielsen, J., Hjortdal, V., Aalkjaer, C., and Boedtkjer, D.B. (2014b). The contribution of K(+) channels to human thoracic duct contractility. Am. J. Physiol. Heart Circ. Physiol. *307*, H33-43.

Telinius, N., Majgaard, J., Kim, S., Katballe, N., Pahle, E., Nielsen, J., Hjortdal, V., Aalkjaer, C., and Boedtkjer, D.B. (2015). Voltage-gated sodium channels contribute to action potentials and spontaneous contractility in isolated human lymphatic vessels. J. Physiol. *593*, 3109–3122.

Thangaswamy, S., Bridenbaugh, E.A., and Gashev, A.A. (2012). Evidence of Increased Oxidative

Stress in Aged Mesenteric Lymphatic Vessels. Lymphat. Res. Biol. *10*, 53–62.

To, K.H.T., Gui, P., Li, M., Zawieja, S.D., Castorena-Gonzalez, J.A., and Davis, M.J. (2020). T-type, but not L-type, voltage-gated calcium channels are dispensable for lymphatic pacemaking and spontaneous contractions. Sci. Rep. *10*, 70.

Trzewik, J., Mallipattu, S.K., Artmann, G.M., Delano, F.A., and Schmid-Schönbein, G.W. (2001). Evidence for a second valve system in lymphatics: endothelial microvalves. FASEB J. Off. Publ. Fed. Am. Soc. Exp. Biol. *15*, 1711–1717.

Tykocki, N.R., Boerman, E.M., and Jackson, W.F. (2017). Smooth Muscle Ion Channels and Regulation of Vascular Tone in Resistance Arteries and Arterioles. Compr. Physiol. *7*, 485–581.

Van, S., Pal, S., Garner, B.R., Steed, K., Sridharan, V., Mu, S., Rusch, N.J., and Stolarz, A.J. (2021). Dantrolene Prevents the Lymphostasis Caused by Doxorubicin in the Rat Mesenteric Circulation. Front. Pharmacol. *12*, 727526.

Veerman, K., Tardiveau, C., Martins, F., Coudert, J., and Girard, J.P. (2019). Single-Cell Analysis Reveals Heterogeneity of High Endothelial Venules and Different Regulation of Genes Controlling Lymphocyte Entry to Lymph Nodes. Cell Rep. *26*, 3116-3131.e5.

Vignes, S., Albuisson, J., Champion, L., Constans, J., Tauveron, V., Malloizel, J., Quéré, I., Simon, L., Arrault, M., Trévidic, P., et al. (2021). Primary lymphedema French National Diagnosis and Care Protocol (PNDS; Protocole National de Diagnostic et de Soins). Orphanet J. Rare Dis. *16*, 18.

Wang, Z., Cui, M., Shah, A.M., Tan, W., Liu, N., Bassel-Duby, R., and Olson, E.N. (2020). Cell-Type-Specific Gene Regulatory Networks Underlying Murine Neonatal Heart Regeneration at Single-Cell Resolution. Cell Rep. *33*, 108472.

Wetterwald, A., Hoffstetter, W., Cecchini, M.G., Lanske, B., Wagner, C., Fleisch, H., and Atkinson, M. (1996). Characterization and cloning of the E11 antigen, a marker expressed by rat osteoblasts and osteocytes. Bone *18*, 125–132.

Wigle, J.T., and Oliver, G. (1999). Prox1 function is required for the development of the murine lymphatic system. Cell *98*, 769–778.

Wigle, J.T., Harvey, N., Detmar, M., Lagutina, I., Grosveld, G., Gunn, M.D., Jackson, D.G., and Oliver, G. (2002). An essential role for Prox1 in the induction of the lymphatic endothelial cell phenotype. EMBO J. *21*, 1505–1513.

Witte, M.H., Erickson, R.P., Luy, L., Brouillard, P., and Vikkula, M. (2021). Human chromosome map of lymphedema-lymphangiogenesis genes: Template for current and future discovery. Lymphology *54*, 167–169.

Wu, T., Hu, E., Xu, S., Chen, M., Guo, P., Dai, Z., Feng, T., Zhou, L., Tang, W., Zhan, L., et al. (2021). clusterProfiler 4.0: A universal enrichment tool for interpreting omics data. Innov. (Cambridge *2*, 100141.

Xu, C., Liu, X., Fang, X., Yu, L., Lau, H.C., Li, D., Liu, X., Li, H., Ren, J., Xu, B., et al. (2022). Single-Cell RNA Sequencing Reveals Smooth Muscle Cells Heterogeneity in Experimental Aortic Dissection. Front. Genet. *13*, 836593.

Zawieja, D.C. (2009). Contractile physiology of lymphatics. Lymphat. Res. Biol. *7*, 87–96.

Zawieja, S.D., Castorena-Gonzalez, J.A., Scallan, J.P., and Davis, M.J. (2018). Differences in L-type Ca(2+) channel activity partially underlie the regional dichotomy in pumping behavior by murine peripheral and visceral lymphatic vessels. Am. J. Physiol. Heart Circ. Physiol. *314*, H991–H1010.

Zawieja, S.D., Castorena, J.A., Gui, P., Li, M., Bulley, S.A., Jaggar, J.H., Rock, J.R., and Davis, M.J. (2019). Ano1 mediates pressure-sensitive contraction frequency changes in mouse lymphatic collecting vessels. J. Gen. Physiol. *151*, 532–554.

Zheng, G.X.Y., Terry, J.M., Belgrader, P., Ryvkin, P., Bent, Z.W., Wilson, R., Ziraldo, S.B., Wheeler, T.D., McDermott, G.P., Zhu, J., et al. (2017). Massively parallel digital transcriptional profiling of single cells. Nat. Commun. *8*, 14049.

Zhou, C., Yahathugoda, C., De Silva, L., Rathnapala, U., Owen, G., Weerasooriya, M., Rao, R.U., Weil, G.J., and Budge, P.J. (2019). Portable infrared imaging for longitudinal limb volume monitoring in patients with lymphatic filariasis. PLoS Negl. Trop. Dis. *13*, e0007762.

Zolla, V., Nizamutdinova, I.T., Scharf, B., Clement, C.C., Maejima, D., Akl, T., Nagai, T., Luciani, P., Leroux, J.C., Halin, C., et al. (2015). Aging-related anatomical and biochemical changes in lymphatic collectors impair lymph transport, fluid homeostasis, and pathogen clearance. Aging Cell *14*, 582–594.

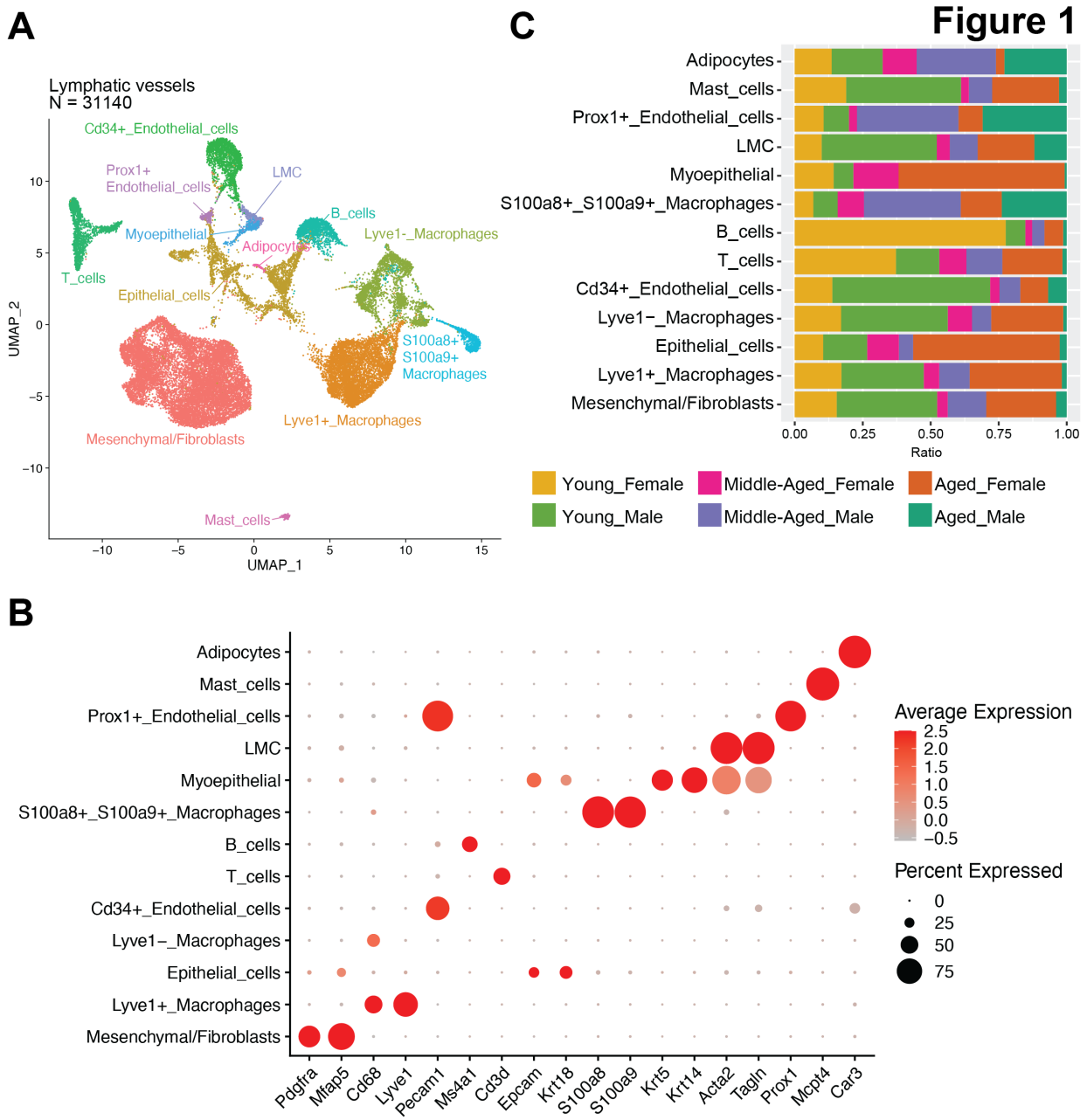

Figure 1. The single-cell atlas of mice collecting lymphatic vessels of various ages.

A) Uniform manifold approximation and projection (UMAP) embedding of 31,140 cells reveals distinct cell types in the collecting lymphatic vessels and adjacent tissues. The collecting lymphatic vessels between inguinal and axillary lymph nodes were isolated from young (6-week-old), middle-age (12-month-old), and aged (18-month-old) mice of both sexes. The lymphatic vessels from 8-10 mice were combined for single-cell RNA sequencing in each age and sex group. **B**) The dot plot represents the gene expression of cell type-specific marker genes. The size of the circle indicates the proportion of cells expressing the selected genes. Red indicates high expression, while gray indicates low expression. Gene expression values are scaled and log-normalized. **C**) The stacked bar plot represents the proportional distribution of cells across different age and sex groups.

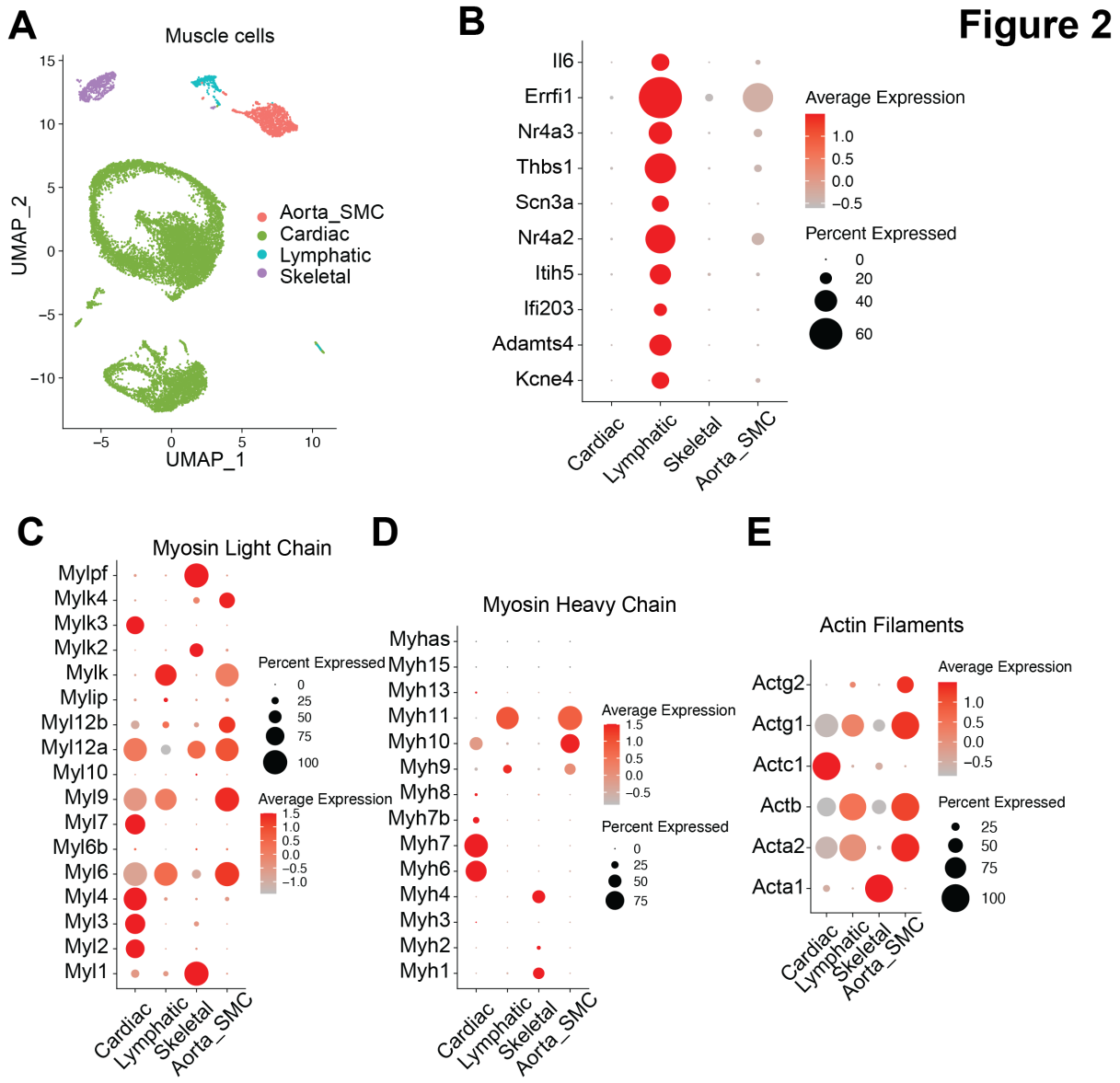

Figure 2. Identify the mouse collecting lymphatic muscle cell-specific marker genes.

A) UMAP embedding of murine LMCs, aortic smooth muscle cells (GSE203594) (Xu et al., 2022), cardiomyocytes (GSE95140, GSE132658, GSE153481) (Goodyer et al., 2022; Nomura et al., 2018; Wang et al., 2020), and skeletal muscle cells (GSE143437) (De Micheli et al., 2020). **B**) The dot plot displays the single-cell gene expression levels of the top 10 most highly differentially expressed genes in LMCs. **C**) The dot plot displays the gene expression of myosin light chain molecules in all the muscle cells. **D**) The dot plot displays the gene expression of myosin heavy chain molecules in all the muscle cells. **E**) The dot plot shows the gene expression of actin filament molecules in all the muscle cells.

Figure 3

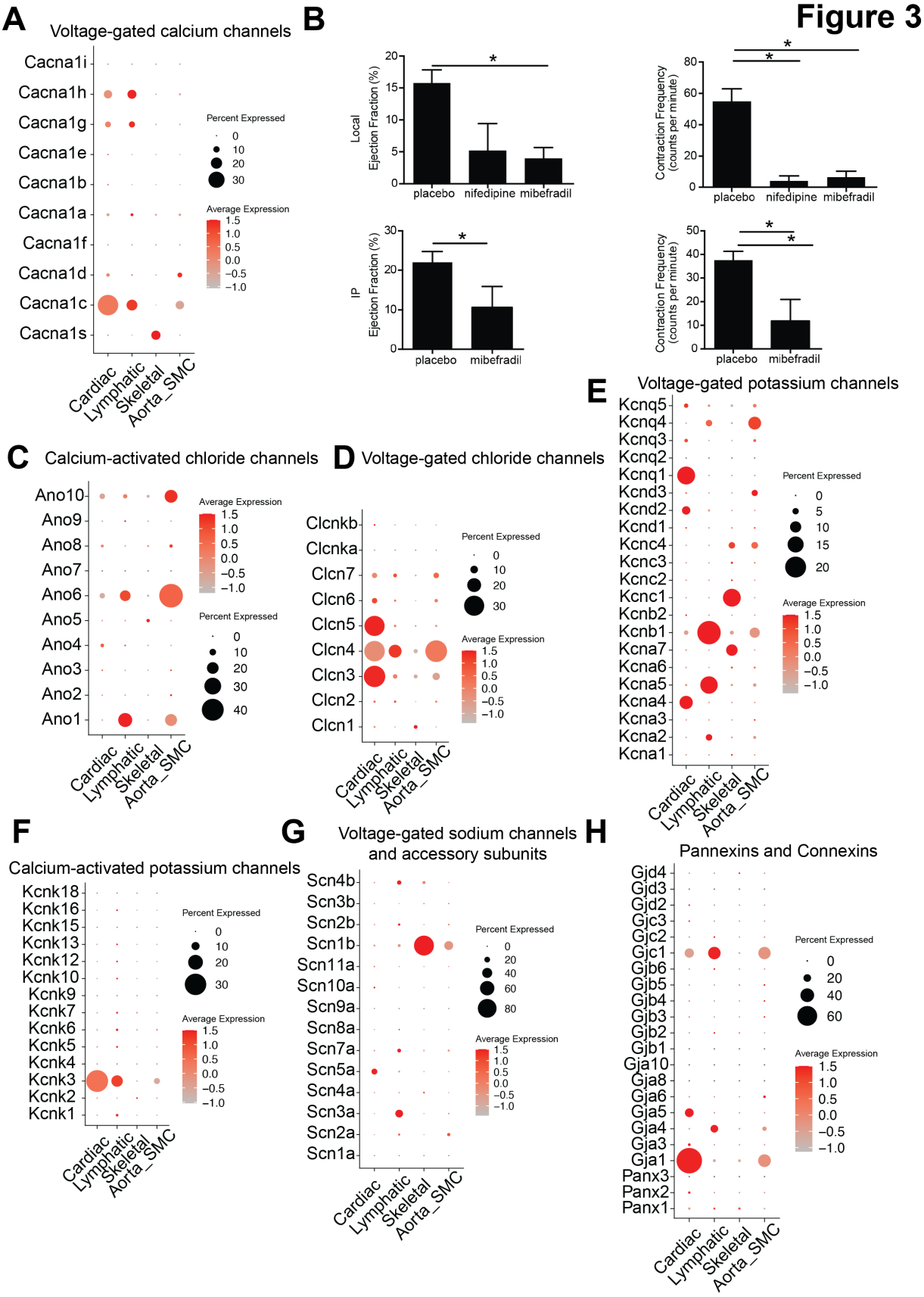
A
Voltage-gated calcium channels
Cacna1i
Cacna1h
Cacna1g
Cacna1e
Cacna1b
Cacna1a
Cacna1f
Cacna1d
Cacna1c
Cacna1s
Cardiac
Lymphatic
Skeletal
Aorta_SMC
Percent Expressed
Average Expression
B
Local Ejection Fraction (%)
IP Ejection Fraction (%)
Contraction Frequency (counts per minute)
placebo
nifedipine
mibefradil
C
Calcium-activated chloride channels
Ano10
Ano9
Ano8
Ano7
Ano6
Ano5
Ano4
Ano3
Ano2
Ano1
D
Voltage-gated chloride channels
Clcnkb
Clcnka
Clcn7
Clcn6
Clcn5
Clcn4
Clcn3
Clcn2
Clcn1
E
Voltage-gated potassium channels
Kcnq5
Kcnq4
Kcnq3
Kcnq2
Kcnq1
Kcnd3
Kcnd2
Kcnd1
Kcnc4
Kcnc3
Kcnc2
Kcnc1
Kcnb2
Kcnb1
Kcna7
Kcna6
Kcna5
Kcna4
Kcna3
Kcna2
Kcna1
F
Calcium-activated potassium channels
Kcnk18
Kcnk16
Kcnk15
Kcnk13
Kcnk12
Kcnk10
Kcnk9
Kcnk7
Kcnk6
Kcnk5
Kcnk4
Kcnk3
Kcnk2
Kcnk1
G
Voltage-gated sodium channels and accessory subunits
Scn4b
Scn3b
Scn2b
Scn1b
Scn11a
Scn10a
Scn9a
Scn8a
Scn7a
Scn5a
Scn4a
Scn3a
Scn2a
Scn1a
H
Pannexins and Connexins
Gjd4
Gjd3
Gjd2
Gjc3
Gjc2
Gjc1
Gjb6
Gjb5
Gjb4
Gjb3
Gjb2
Gjb1
Gja10
Gja8
Gja6
Gja5
Gja4
Gja3
Gja1
Panx3
Panx2
Panx1

Figure 3. The presence of ion channel molecules in LMCs. A) The dot plot shows the gene expression of calcium channel molecules in all the muscle cells. **B**) The lymphatic vessel ejection fraction and contraction frequency after local or systemic administration of calcium blockers. Nifedipine is a L-type calcium channel blocker. Mibefradil is a T-type calcium channel blocker. **C-H**) The dot plot shows the gene expression of C) calcium-activated chloride channels, D) voltage-gated chloride channels, E) voltage-gated potassium channels, F) calcium-activated potassium channels, G) sodium channels and accessory subunits, and H) pannexins and connexins in all the muscle cells.

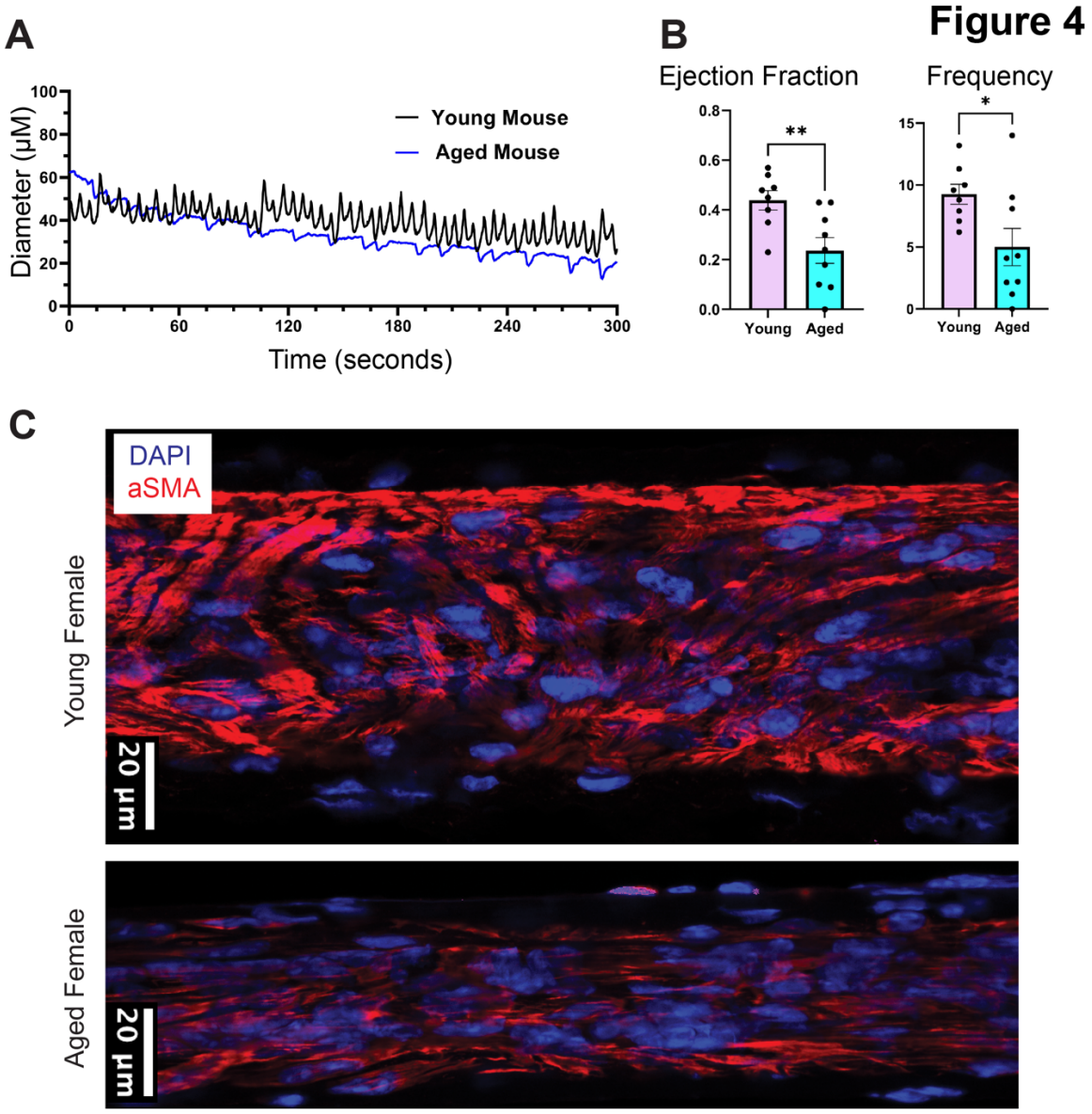

Figure 4. The collecting popliteal lymphatic vessels exhibit diminished contraction and muscle cell coverage during aging.

A) Representative recording of lymphatic vessel diameter changing over time in a young (6 weeks) and aged (18 months) mouse. **B**) The lymphatic pumping ejection fraction and contraction frequency (cycles/min) in young and aged mice. The ejection fraction for young mice was 0.44 +/- 0.04 (mean +/- SEM), and for aged mice was 0.24 +/- 0.05 (mean +/- SEM), with a mean difference of 0.20 +/- 0.07 (P = 0.008). The frequency for young mice was 9.3 +/- 0.8 (mean +/- SEM, cycles/min), and for aged mice was 5.1 +/- 1.5 (mean +/- SEM, cycles/min), with a mean difference of 4.3 +/- 1.8 cycles/min (P = 0.03). Student's t-test was used to compare the means between two groups. **C**) Representative whole mount immunofluorescence image of αSMA in lymphatic vessel segments of young (6 weeks) and aged (18 months) C57BL/6 female mice. The scale bar represents 20 μm.

Figure 5

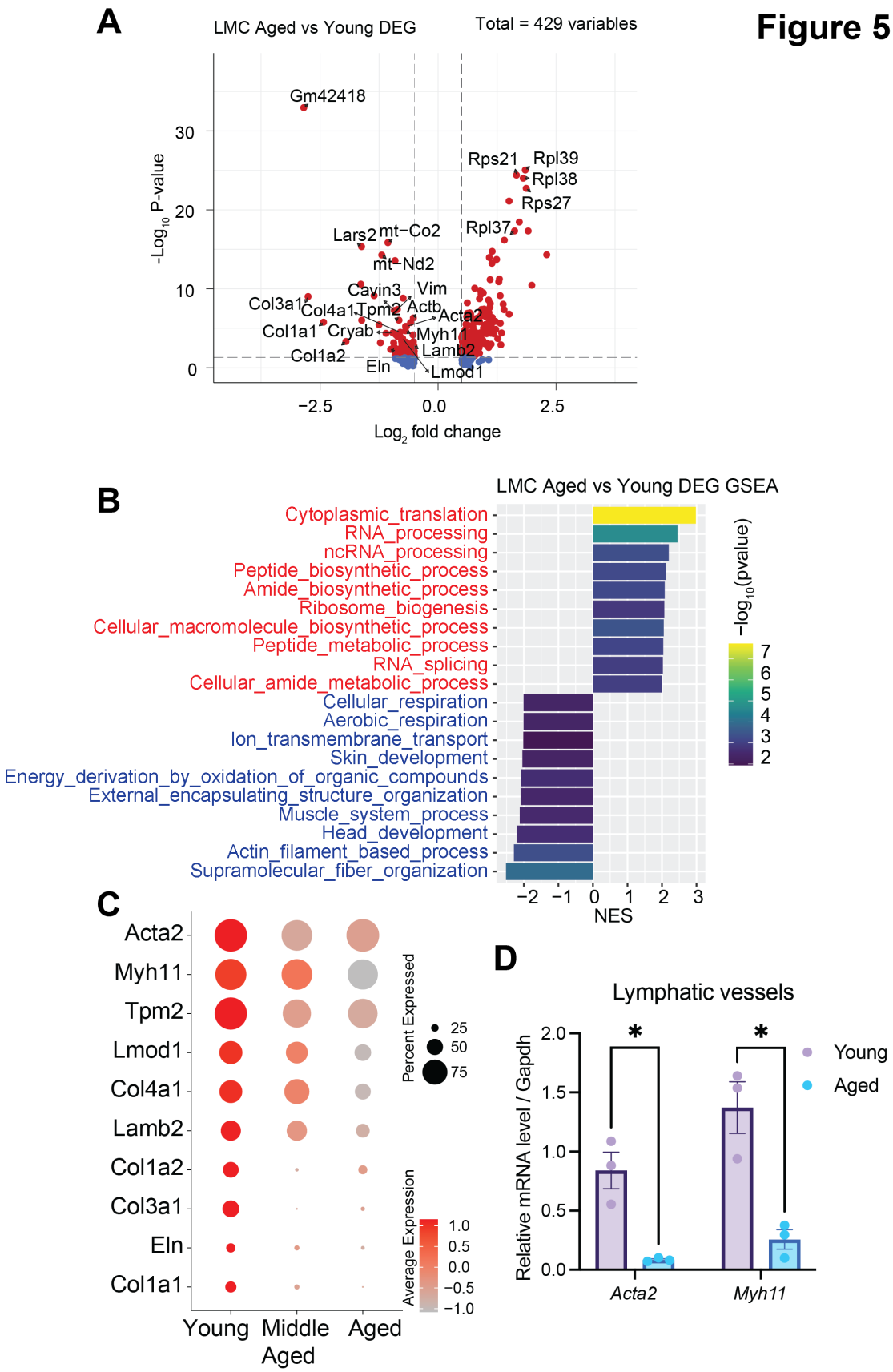
A
LMC Aged vs Young DEG
Total = 429 variables
Gm42418
Rps21
Rpl39
Rpl38
Rps27
Rpl37
Lars2
mt−Co2
mt−Nd2
Cavin3
Vim
Col3a1
Col4a1
Tpm2
Actb
Acta2
Col1a1
Cryab
Myh11
Lamb2
Col1a2
Eln
Lmod1
-Log10 P-value
Log2 fold change
B
LMC Aged vs Young DEG GSEA
Cytoplasmic_translation
RNA_processing
ncRNA_processing
Peptide_biosynthetic_process
Amide_biosynthetic_process
Ribosome_biogenesis
Cellular_macromolecule_biosynthetic_process
Peptide_metabolic_process
RNA_splicing
Cellular_amide_metabolic_process
Cellular_respiration
Aerobic_respiration
Ion_transmembrane_transport
Skin_development
Energy_derivation_by_oxidation_of_organic_compounds
External_encapsulating_structure_organization
Muscle_system_process
Head_development
Actin_filament_based_process
Supramolecular_fiber_organization
NES
−log10(pvalue)
C
Acta2
Myh11
Tpm2
Lmod1
Col4a1
Lamb2
Col1a2
Col3a1
Eln
Col1a1
Young
Middle Aged
Aged
Percent Expressed
Average Expression
D
Lymphatic vessels
Relative mRNA level / Gapdh
Young
Aged
Acta2
Myh11

Figure 5. Characterization of murine lymphatic smooth muscle cells during aging.

A) The volcano plot represents the differentially expressed genes in LMCs between the young (6-week-old) and aged (18-month-old) groups. The red dots indicate significant differentially expressed genes with a fold change > 0.5 and P value <0.05. **B)** Gene set enrichment analysis (GSEA) of significant differentially expressed genes in LMCs between young (6-week-old) and aged (18-month-old) mice. The gene ontology biological process gene sets were used as a reference for the GSEA analysis. The gene sets are ordered by normalized enrichment score (NES), and the bar plot displays the top 10 up- or down-regulated gene sets. Positive values of NES show higher expression in aged LMCs, and negative values of NES show higher expression in young LMCs. **C)** The dot plot represents the gene expression of muscle cell contractile-associated genes in LMCs. The size of the circle indicates the proportion of cells expressing the selected genes. Red indicates high expression, while gray indicates low expression. Gene expression values are scaled and log-normalized. **D**) The gene expression of *Acta2* and *Myh11* in collecting lymphatic vessels in young (6-week-old) and aged mice (18-month-old) was quantified by real-time PCR. In each group, the lymphatic vessels were isolated from one male mouse and one female mouse, which were combined for RNA extraction. Student's t-test was used to compare the means between two groups. *p<0.05.

Figure 6

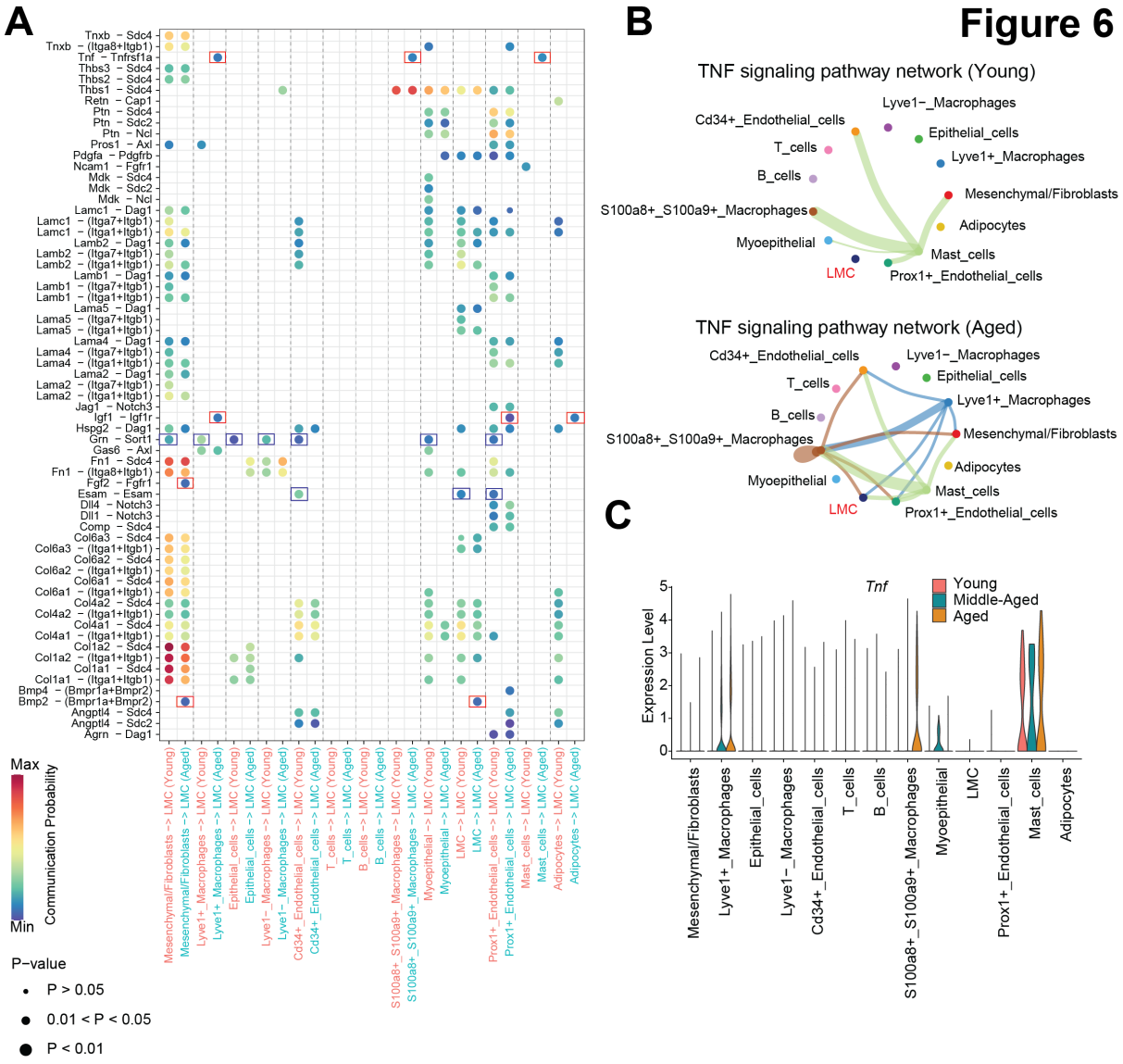
A
B
TNF signaling pathway network (Young)
Lyve1−_Macrophages
Cd34+_Endothelial_cells
Epithelial_cells
T_cells
Lyve1+_Macrophages
B_cells
Mesenchymal/Fibroblasts
S100a8+_S100a9+_Macrophages
Adipocytes
Myoepithelial
Mast_cells
LMC
Prox1+_Endothelial_cells
TNF signaling pathway network (Aged)
C
Tnf
Young
Middle-Aged
Aged
Expression Level
Mesenchymal/Fibroblasts
Lyve1+_Macrophages
Epithelial_cells
Lyve1−_Macrophages
Cd34+_Endothelial_cells
T_cells
B_cells
S100a8+_S100a9+_Macrophages
Myoepithelial
LMC
Prox1+_Endothelial_cells
Mast_cells
Adipocytes
Max
Min
Communication Probability
P−value
P > 0.05
0.01 < P < 0.05
P < 0.01

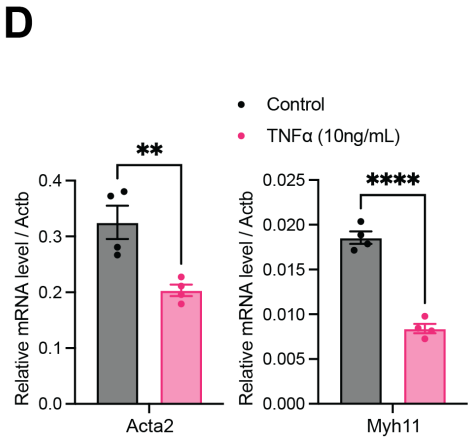
D
Control
TNFα (10ng/mL)
**
****
Relative mRNA level / Actb
Acta2
Myh11

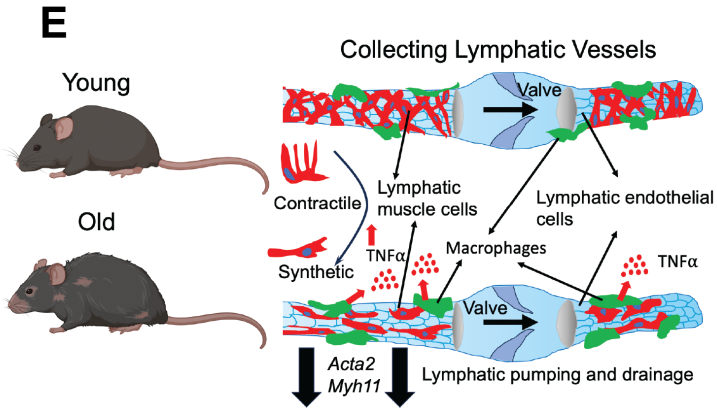
E
Young
Old
Collecting Lymphatic Vessels
Valve
Contractile
Lymphatic muscle cells
Lymphatic endothelial cells
Synthetic
TNFα
Macrophages
Acta2
Myh11
Lymphatic pumping and drainage

Figure 6. The cell-cell interactions between cells that comprise lymphatic vessels and cells in adjacent tissues.

A) Dot plot describing the ligand-receptor interactions between cells of the lymphatic vessels and adjacent tissue (source) and muscle cells (target) in young (6-week-old) and aged (18-month-old) mice. The size of the circle represents the p-value of the communications. The color of the dot represents the communication probability of the ligand-receptor pair between cells. Blue represents low probability, and red represents high probability. The red box highlights the ligand-receptor pairs that were elevated in the aged (18-month-old) mice, blue box highlights the ligand-receptor pairs that were decreased in the aged (18-month-old) mice. **B**). The network of cell-cell communication in TNFα signaling pathway in young (6-week-old) and aged (18-month-old) mice. **C**) The violin plot shows the gene expression of *Tnf* in all the cells of various ages. **D**) The gene expression of *Acta2* and *Myh11* in lymphatic muscle cells after TNFα treatment. The lymphatic muscle cells were collected from the afferent lymphatic vessel to the popliteal lymph node of young (6-week-old) mice and cultured in the presence of 10 ng/mL TNFα for 48 hours. **E**) Macrophages and mast cells positioned in the microenvironment of aged lymphatic vessels produce TNFα, which suppresses the gene expression of *Acta2*, *Myh11* and other contractile apparatus-related genes and drives the contractile to synthetic transition of LMCs. The reduction of LMC coverage and decreased contractile phenotype in aged lymphatic vessels lead to a lower ejection fraction and contraction frequency. ** $p < 0.01$; **** $p < 0.0001$.